U.S. DEPARTMENT OF ENERGY

PNNL-23179
DSGREP-RPT-004, Rev. 0

Prepared for the U.S. Department of Energy
under Contract DE-AC05-76RL01830

Morphology of Gas Release in Physical Simulants

RC Daniel
CA Burns
AD Crawford
LR Hylden
SA Bryan
PJ MacFarlan
PA Gauglitz

March 2014

Pacific Northwest
NATIONAL LABORATORY

Proudly Operated by Battelle Since 1965

DISCLAIMER

PACIFIC NORTHWEST NATIONAL LABORATORY
operated by
BATTELLE
for the
UNITED STATES DEPARTMENT OF ENERGY
under Contract DE-AC05-76RL01830

Printed in the United States of America

Available to DOE and DOE contractors from the
Office of Scientific and Technical Information,
P.O. Box 62, Oak Ridge, TN 37831-0062;
ph: (865) 576-8401
fax: (865) 576-5728
email: reports@adonis.osti.gov

Available to the public from the National Technical Information Service
5301 Shawnee Rd., Alexandria, VA 22312
ph: (800) 553-NTIS (6847)
email: orders@ntis.gov <http://www.ntis.gov/about/form.aspx>
Online ordering: http://www.ntis.gov


This document was printed on recycled paper.
(8/2010)

PNNL-23179
DSGREP-RPT-004, Rev. 0

Morphology of Gas Release in Physical Simulants

RC Daniel
CA Burns
AD Crawford
LR Hylden
SA Bryan
PJ MacFarlan
PA Gauglitz

March 2014

Prepared for
the U.S. Department of Energy
under Contract DE-AC05-76RL01830

Pacific Northwest National Laboratory
Richland, Washington 99352

Executive Summary

This report documents testing activities conducted as part of the Deep Sludge Gas Release Event Project (DSGREP). The testing described in this report supports evaluations of the potential retention and release mechanisms of hydrogen bubbles in underground radioactive waste storage tanks at Hanford. The primary goal of the testing was to evaluate the rate, extent, and morphology of gas release in simulant materials. Previous, undocumented scoping tests have shown dramatically different gas release behaviors from simulants with similar physical properties. Specifically, previous gas release tests have evaluated the extent of release of 30 Pa kaolin and 30 Pa bentonite clay slurries. While both materials are clays and both have equivalent material shear strength using a shear vane, it was found that upon stirring, gas was released immediately and completely from bentonite clay slurry while little if any gas was released from the kaolin slurry. The current work replicated the undocumented kaolin and bentonite clay tests in a controlled quality test environment and evaluated gas release in another simulant recently used in DSGREP testing. Overall, three simulant materials were evaluated: 1) a 30 Pa kaolin clay slurry, 2) a 30 Pa bentonite clay slurry, and 3) Rayleigh-Taylor (RT) Simulant (a simulant designed to support DSGREP RT instability testing[1]). Entrained gas was generated in the simulant materials using two methods: 1) application of vacuum over about a 1-minute period to nucleate dissolved gas within the simulant and 2) addition of hydrogen peroxide to generate gas by peroxide decomposition in the simulants over about a 16-hour period. Bubble release was effected by vibrating the test material using an external vibrating table. When testing with hydrogen peroxide, gas release was also accomplished by stirring of the simulant.

Table S.1 provides the matrix of tests supporting the test activities documented in this report. For tests where gas was generated by application of vacuum, two test strategies were employed: one where bubbles were grown at 50 torr (to whatever ultimate gas fraction could be achieved at this vacuum pressure) and another where bubbles were grown until the total fraction of entrained gas was approximately 15%. Gas fractions generated using 50 torr vacuum ranged from 18 to 24 vol%, whereas gas fractions in experiments targeting 15 vol% entrained gas realized gas fractions ranging from 13 to 18 vol%. Tests performed under vacuum with vibration as the primary means of gas release found that all simulants partially release entrained gas. However, bentonite clay demonstrated strong retention of approximately 5% to 10% gas after the primarily release. Vibration removed the bulk of entrained gas from kaolin clay, where RT Simulant typically showed rapid and near complete release of gas relative to the two other simulants. In all cases, gas release appeared to be affected by bubble coalescence, which allowed the bubbles to grow and rise more rapidly (under the influence of buoyancy) through the test material. Large releases were observed to correspond with the rise of bubbles from the bottom of the test collection. The results indicated that gas release was more complete when the initial fraction of gas entrained in the slurry is high. Increased gas content is postulated to favor bubble coalescence, which drives the release process, as well as provide more extensive shearing of the slurry, leading to greater shear-induced motion and release of bubbles (similar to that observed in bubble cascade release events.

[1] Rassat SD, PA Gauglitz, LA Mahoney, RP Pires, DR Rector, JA Fort, GK Boeringa, DN Tran, MR Elmore, and WC Buchmiller. 2013. *Gas Release Due to Rayleigh-Taylor Instability within Sediment Layers in Hanford Double-Shell Tanks: Results of Scaled Vessel Experiments, Modeling, and Extrapolation to Full Scale*. PNNL-23060 (DSGREP-RPT-002, Rev. 0), Pacific Northwest National Laboratory, Richland, Washington

The observed bubble release behavior under vacuum was different from the results of the scoping tests that motivated the current test activities. Specifically, scoping tests with bubbles generated by hydrogen peroxide decomposition found near complete release of gas from 30 Pa bentonite clay and retention of gas by 30 Pa kaolin clay. Current tests with bubbles generated by application of vacuum found near complete release of gas from kaolin and only partial release of gas from bentonite. There are several differences in the scoping and DSGREP bubble release tests that could explain the difference in gas release behaviors. The difference in generation methods could cause differences in bubble size and count or addition of peroxide could alter the clay chemistry. Either phenomenon could lead to different bubble release behaviors. Second, the test containers have different aspect ratios. Scoping tests used wide (~20 cm) 2 L beakers, whereas current testing used a 5 cm (internal diameter) column. It is possible that the increased bubble-wall interactions in the current testing altered the release behavior. Finally, scoping and current gas release tests used different release mechanisms. Scoping tests disrupted bubbles by stirring with a spatula (~2.5 cm wide), whereas current tests used a vibrating table. Differences in the amplitude of disruption (up to ±100 mm with the spatula versus ±1 mm with the table) and frequency of disruption (~1 Hz with the spatula stirring versus ~50 Hz with the table) could lead to different release behaviors. Whatever the cause, the results of 50 torr vacuum testing provided motivation to perform the confirmatory tests with peroxide discussed in the report.

To determine the cause of the discrepancy between gas release behaviors in scoping tests and the vacuum tests, gas generation and release tests in all three simulants were repeated using hydrogen peroxide as the gas generation mechanism. These tests confirmed the release behavior observed in the scoping tests that motivate the current test activities. Specifically, the hydrogen peroxide tests indicate that, when bubbles are formed using hydrogen peroxide decomposition over long growth periods (i.e., 16 hours) to a target initial gas fraction of 15 vol%, shear or vibration of:

- 30 Pa bentonite clay slurry releases gas immediately and to a significant, but not complete, extent (with final gas hold-up ranging from 1 to 3 vol%)
- 30 Pa kaolin clay slurry releases gas slowly and to a minimal extent (with final gas hold-up ranging from 8 to 12 vol%)
- 30 Pa RT Simulant effects a release that, in terms of rate, falls between that of kaolin and bentonite, and that, in terms of extent, is comparable to that of bentonite.

As discussed above, there are several differences in vacuum and hydrogen peroxide release tests that could cause the difference in gas release behaviors. First, the difference in gas generation methods could result in differences in bubble size distribution and count or addition of peroxide could alter the simulant chemistry/rheology. Observation of bubbles at the wall appears to confirm that hydrogen peroxide produces an entrained gas morphology different from vacuum testing, at least in 30 Pa kaolin and 30 Pa RT Simulant. Specifically, use of hydrogen peroxide produced spherical bubbles with radial cracks[1] in kaolin and RT Simulant, whereas use of a vacuum only produces small (on the order of 1 mm and smaller), spherical bubbles. In addition, both 30 Pa kaolin and RT Simulant dewatered when testing with hydrogen peroxide, likely as a result of solids settling over the long bubble growth period (16 hours in hydrogen peroxide testing relative to 1 to 15 minutes in vacuum testing). Use of hydrogen peroxide did not noticeably alter bubble morphology in bentonite clay relative to vacuum testing; both methods only

[1] Visual observation was unable to determine if the cracks were filled with gas or water.

produce small spherical bubbles. Use of hydrogen peroxide did not appear to drastically alter the shear strength of the test materials. Shear strength measurements were made on simulants with added hydrogen peroxide immediately before disruption; all fell within the acceptable test range of 15 to 45 Pa and were generally around 20 to 30 Pa.

Table S.1. Matrix of Bubble Generation and Release Studies for Gas Generation and Release Morphology Testing

Simulant Material	Gas Generation Method	Test Vessel	No. of Tests
30 Pa kaolin	Vacuum (at 50 torr)	Sealed Test Column	3
	Vacuum (to 15% Gas Volume)	Sealed Test Column	3
	Hydrogen Peroxide	2 L Beaker	1
	Hydrogen Peroxide	Primary Test Apparatus	1
	Hydrogen Peroxide	100 mL Graduated Cylinder	1
30 Pa bentonite	Vacuum (at 50 torr)	Sealed Test Column	3
	Vacuum (to 15% Gas Volume)	Sealed Test Column	3
	Hydrogen Peroxide	2 L Beaker	1
	Hydrogen Peroxide	Primary Test Apparatus	1
	Hydrogen Peroxide	100 mL Graduated Cylinder	1
30 Pa RT Simulant	Vacuum (at 50 torr)	Sealed Test Column	3
	Vacuum (to 15% Gas Volume)	Sealed Test Column	3
	Hydrogen Peroxide	2 L Beaker	1
	Hydrogen Peroxide	Primary Test Apparatus	1
	Hydrogen Peroxide	100 mL Graduated Cylinder	1
Total			27

It could also be postulated that differences in the geometry of the test container or method of gas release (vibration versus stirring) yield the differences in release behavior observed between hydrogen peroxide and vacuum testing. Specifically, scoping tests used wide (~20 cm) 2 L beakers with stirring as the release mechanism, whereas current vacuum testing used a 5 cm (internal diameter) column with vibration as a gas release mechanism. To evaluate the influence of test container geometry and release mechanism on gas release, hydrogen peroxide tests were repeated in the primary test apparatus (used for vacuum testing) and in a smaller diameter 100 mL graduated cylinder, with bubble release affected by vibration. In general, these tests found that the gas release behaviors did not depend strongly on test container geometry or on release mechanism (vibration versus stirring) such that the gas release profiles mirrored those for the 2 L hydrogen peroxide stir tests.

For these reasons, it can be postulated that the difference in release behaviors observed between vacuum and hydrogen peroxide testing primarily derives from the method of gas generation itself (and how nucleation of dissolved gas or decomposition of hydrogen peroxide impacts local simulant chemistry) or on the length of time required to grow bubbles (several minutes using vacuum versus up to 16 hours when using hydrogen peroxide). In terms of shear strength, several differences are notable between vacuum and hydrogen peroxide testing. For vacuum testing, shear strength is similar among test simulants, and here, the strongest simulant, kaolin at ~25 Pa, releases more completely than the relatively

weaker ~18 Pa bentonite slurry. When testing with hydrogen peroxide, bentonite clay slurry shear strength (which at 22 Pa is nearly unchanged relative to that realized in vacuum testing) falls below that measured for kaolin (36 Pa) and RT Simulant (38 Pa). The cause of increase in the shear strength of kaolin and RT Simulant slurries over that achieved in vacuum testing can be attributed to reaction of the simulant with hydrogen peroxide or, more likely, by compaction (and increased solids concentration of the slurry) as a result of settling and dewatering. In terms of observed gas release behaviors, the weakness of the bentonite slurry in hydrogen peroxide testing (relative to kaolin and RT Simulant) could explain the rapid release of entrained gas from bentonite relative to other test simulants. However, reliance on shear strength alone does not explain why the similar strength bentonite slurry does not release rapidly or to the same extent in vacuum testing, nor does it explain why the 38 Pa RT Simulant releases more quickly and to a greater extent than the 36 Pa kaolin slurry when testing with hydrogen peroxide. As such, while material strength may play a role in the release behavior, other equally important mechanisms appear to control that rate and extent of gas release.

It is expected that different gas generation and growth mechanisms (i.e., vacuum versus hydrogen peroxide) will result in different entrained bubble count, morphology, and size. Qualitative analysis of gas morphology, by observing entrained gas at the container walls, finds that vacuum testing produces spherical bubbles in all test simulants whereas hydrogen peroxide produces bubbles in bentonite slurries and bubbles with radial cracks in kaolin and RT Simulant slurries. Current assessment of bubble morphology should be approached with caution, as it presumes that the bubble morphology observed at the container walls is representative of the internal bubble morphology (which could not be visually assessed because all test slurries were opaque). Regardless of this limitation, it is likely that differences in the bubble size distribution across simulants and between gas generation methods will drive differences in the how bubbles and gas pockets coalesce with one another, rise through, and are expelled from the test simulant. Assessment of entrained gas morphology in the current study did not attempt to quantify differences in bubble count and size distribution across test simulants and gas generation methods. If the differences observed in vacuum and hydrogen peroxide release tests need to be resolved, then future tests should consider quantification of bubble structure within the test simulant for each gas generation mechanism.

Overall, the test results suggest that caution should be exercised when selecting the bubble generation and simulant disturbance methods when evaluating the gas release behaviors. The results of this study indicate that bubble nucleation and growth by application of a vacuum and subsequent release by vibration do not replicate gas release behaviors obtained by hydrogen peroxide decomposition and subsequent stirring. Indeed, the gas release behaviors obtained in vacuum and vibration testing is the reverse of that obtained when testing with hydrogen peroxide. These differences suggest a strong dependence of the gas release behaviors on the mechanism used to form the bubbles in situ. Further development of simulants and gas generation mechanisms for release testing should evaluate the reasonableness of gas release morphology against that observed in actual wastes.

Acknowledgments

The authors would like to thank Matt Edwards and Quality Engineer Bill Dey for their careful and thorough review of this document and supporting calculations. The authors would like to thank Matt Wilburn for document preparation and technical editing. Finally, the authors would like to thank Washington River Protection Solutions for funding the work documented in this report.

Acronyms and Abbreviations

ASO	Analytical Support Operations
DSGREP	Deep Sludge Gas Release Event Project
HEPA	high-efficiency particulate air
M&TE	measuring and testing equipment
PNNL	Pacific Northwest National Laboratory
PTFE	polytetrafluoroethylene
QA	quality assurance
RCW	Richland city water
RT	Rayleigh-Taylor (instability)
WWFTP	Washington River Protection Solutions LLC Waste Form Testing Program

Contents

Figures

Tables

1.0 Introduction

In Hanford underground waste storage tanks, a typical waste configuration is a settled bed of solid particles with interstitial liquid beneath a supernatant liquid layer. The settled bed is typically also composed of layers that can have different physical and chemical properties. One postulated configuration within the settled bed is a more-dense layer lying atop a less-dense layer. The different densities can be a result of different gas retention in the layers, different degrees of settling and compaction in the layers, or different solid particle compositions. Such a configuration can experience a Rayleigh-Taylor (RT) instability, in which the less-dense lower layer rises into the upper layer, and this motion may cause a release of retained gas. Until the recent preliminary study of Gauglitz et al. (2013), studies of gas retention and release in Hanford waste had not considered potential buoyant motion within a settled bed of sludge solids. One purpose of the Deep-Sludge Gas Release Event Project (DSGREP) at Pacific Northwest National Laboratory (PNNL) is to provide quantitative information for estimating the size of gas release events from sludge waste stored in double-shell tanks should an RT instability occur. A second purpose of the DSGREP is to demonstrate that gas retention behavior in deep sludge layers is essentially unaffected by the depth of the sludge layer.

The goal of testing performed is to study the rate, extent, and morphology of gas release from different sludge simulants with similar rheology (i.e., shear strength). Previous work has found different release mechanics for clay slurries that have equal shear strength (both 30 Pa) but are composed of different types of clay (kaolin and bentonite). In these previous experiments, a 30 Pa kaolin in water clay slurry and a 30 Pa bentonite in water slurry were prepared and placed into separate tests containers. Hydrogen peroxide solution was mixed into the clay slurries at low concentrations. Hydrogen peroxide decomposes, producing gas that is held within the clay matrix when the buoyant force of the gas bubbles (or other gas pocket morphology, such as slits and cracks) is insufficient to overcome the yield stress of the clay. The peroxide reaction is also slow, such that the gas bubbles grow with time until they become large enough to overcome the material yield stress (leading to a bubble release event) or until the supply of peroxide is exhausted. In previous clay tests, bubble formation was allowed to occur until approximately 15 vol% of gas was trapped in the clay matrix. The gas was then forcibly released by stirring the clay/gas mixture with a spatula. Application of shear yields the clay, allowing bubbles to rise as a result of buoyancy. Mixing also facilitates bubble coalescence, which further accelerates the release process. When performed on the 30 Pa kaolin clay and 30 Pa bentonite clay slurries, the test described above finds different release behaviors for the two clays:

- **30 Pa bentonite clay:** Rapid release of all the entrained gas (i.e., within several seconds) is observed near the stirred region. If the entire container of bentonite is stirred, all gas is released rapidly.
- 3**0 Pa kaolin clay:** Limited release of entrained gas is observed in the stirred region. Bubbles will remain in the clay matrix, and while they may move with the clay when stirred, they do not appreciably coalescence or rise to the surface.

Given that gas release is expected to be a strong function of yield stress and has been correlated with a gravity yield parameter (Laxton and Berg 2005; Gauglitz et al. 2010; Epstein and Gauglitz 2010; Gauglitz et al. 2012), the difference in gas release observed for the two clay simulants, each with similar yield stress, highlights the value of evaluating gas release morphology (i.e., the rate and extent of release) across different physical and chemical simulants. Such evaluations could help establish the representativeness of gas release from a given simulant against that which could potentially occur in

settled sludges in the Hanford tank farm. The current study evaluates gas release in three physical simulant materials that have been used for gas release testing. Simulants to be tested included

- kaolin clay slurry
- bentonite clay slurry
- Rayleigh-Taylor test slurry [a dry solid mixture of 90 wt% silica (Min-U-Sil 30) and 10 wt% bentonite slurried in water]

The test results provide a reference against which existing and future gas-release tests with Hanford waste sludges can be evaluated.

The objective of the current study was to study the rate, extent, and morphology of gas release from the three sludge simulants. As part of this effort, RT Simulant gas release will be compared to that from the previously tested kaolin and bentonite clay slurries. In addition, because the 30 Pa bentonite/kaolin scoping tests that motivated this study were neither captured under a rigorous nuclear quality program (equivalent to the QA program implemented for the DSGREP testing) nor documented in a formal PNNL report, a secondary objective of the revised testing was to repeat the kaolin and bentonite release tests so that they could be formally documented and qualified.

It is important to note that the current studies, as originally planned, were intended to support development of a gas generation and release test apparatus for hot-cell testing of actual waste sludge. The experimental design focused on a gas-generation and release system that 1) could be operated by remote manipulation (i.e., could be tested in a hot-cell environment), 2) would employ a gas-generation mechanism that would not substantially alter the chemistry of the test material and that would allow gas to be regenerated reproducibly over several gas generation and release cycles, and 3) would maximize replicate testing potential with a very limited volume of test sample (~250 to 500 mL by volume). Although no hot-cell work with actual waste material was conducted as part of the final experimental activities, the hot-cell test apparatus was used to support cold simulant testing with the intent of providing facilitating comparison against future hot-cell work (which will likely use a similar test apparatus). As such, the experimental design, apparatus, and test process used in the current study differ significantly from non-radiological methods used to generate and release bubbles in other DSGREP tasks and historically (e.g., Rassat and Gauglitz 1995; Rassat et al. 2013).

This report documents experimental activities by evaluating the gas generation and release morphology of simulant materials used in DSGREP testing. The objectives of the study are provided in Section 2.0. The DSGREP quality requirements are outlined in Section 3.0. The test equipment and simulant materials are described in Section 4.0. Test results for simulant gas-generation and release testing are discussed in Section 5.0. Conclusions and recommendations are provided in Section 6.0.

2.0 Objectives

The primary objectives of gas generation and release morphology testing are documented in Test Plan TP-DSGREP-013.[1] Experimental activities described herein satisfy, in part, the TP-DSGREP-013 objectives to "[compare] the bubble release behavior of simulants". No hot-cell testing of actual waste sludge was performed for TP-DSGREP-013, and as such, release behavior will only be compared among simulants. The specific experimental objectives addressed in this report are:

- compare the bubble release behavior (i.e., measure and compare rate, extent, and morphology of gas release from) of simulants composed of kaolin in water, bentonite in water, and a 90:10 mixture of Min-U-Sil 30 and bentonite in water (this simulant is used in the Rayleigh-Taylor gas release tasks)
- verify previously un-released test results indicating different release behaviors in kaolin and bentonite clay slurries and capture these results in a controlled quality environment.

These measurements will provide a basis for comparing release behavior among simulants and provide a reference against which future simulant or actual waste release behavior may be gaged.

It should also be noted that experimental design efforts associated with TP-DSGREP-013 supported development of a method for "quantifying bubble generation and release compatible with [actual waste sludge]". Gas release tests associated with development of the test apparatus are not documented in this report. However, this objective strongly influenced the gas generation method and test equipment employed herein and, for this reason, attention is given to compatibility of gas generation and release techniques with hot-cell testing environments when discussing the material and test equipment (Section 4.0).

[1] Daniel R. 2013. Test Plan TP-DSGREP-013, Rev. 0.0 (or current revision). *Gas Release Testing in AY-102 Sludge*. Pacific Northwest National Laboratory, Richland, Washington.

3.0 Quality Assurance

DSGREP staff perform work in accordance with the document *Support to Evaluation of Gas Release Mechanisms in Deep Sludge Project Quality Assurance Plan* (64405-QA-001). The DSGREP uses the Washington River Protection Solutions LLC Waste Form Testing Program (WWFTP) QA program plan (QA-WWFTP-001) at the Applied Research level as the basis for performing work. The WWFTP QA program implements an NQA-1-2000 Quality Assurance Program, graded on the approach presented in NQA-1-2000, Part IV, Subpart 4.2. This QA program and implementing procedures meet the quality requirements of NQA-1-2004, NQA-1a-2005, and NQA-1b-2007 as provided in the Statement of Work authorizing PNNL to conduct these studies.[1] When needed, analyses performed by the Analytical Support Operations (ASO) organization are conducted under the ASO QA Plan, which complies with the requirements of the Hanford Analytical Services Quality Assurance Requirements Document and NQA-1.

Table 3.1 lists the implementing procedures identified in the WWFTP QA program plan (QA-WWFTP-001) that governs the work conducted under this study. Listed below is a summary of key procedures.

- All staff members contributing to the work described in this report received proper technical and QA training prior to commencing quality-affecting work in accordance with QA-NSLW-0201, *Training.*
- The planned studies were conducted in accordance with QA-NSLW-1102, *Scientific Investigation for Applied Research*.
- The studies were planned and conducted in accordance with QA-NSLW-1104, *Test Plans*, and QA-NSLW-1107, *Test Instructions*.
- Test materials and samples were identified and controlled in accordance with QA-NSLW-0801, *Item Identification and Sample Control*.
- Measuring and testing equipment (M&TE) used to generate quality-affecting data was properly procured, controlled, calibrated, handled, and maintained in accordance with QA-NSLW-1201, *Calibration and Control of M&TE*.
- All data and calculations used in this report were reviewed in accordance with QA-NSLW-1108, *Data Entry and Data Review*, QA-NSLW-0301, *Management of Electronic Data*, and QA-NSLW-0304, *Calculations.*
- This technical report was generated in accordance with QA-NSLW-1109, *Reporting*, and was peer reviewed in accordance with QA-NSLW-0601, *Document Preparation and Change*, and QA-NSLW-0603, *Independent Technical Review*.

[1] This program has been independently evaluated by Acquisition Verification Services of Mission Support Alliance to specified requirements of NQA-1-2004 (including NQA-1a-2005 and NQA-1b-2007 Addenda) and is operating under a Washington River Protection Solutions-approved Supplier Quality Assurance Program Implementation Plan (QA-WWFTP-002).

Table 3.1. QA Implementing Procedures (from QA-WWFTP-001)

Document Number	Title
QA-NSLW-0201	*Training*
QA-NSLW-0202	*Surveillances*
QA-NSLW-0203	*Management Assessments*
QA-NSLW-0301	*Management of Electronic Data*
QA-NSLW-0302	*Software Control – Applied Research*
QA-NSLW-0304	*Calculations*
QA-NSLW-0305	*Safety Software*
QA-NSLW-0401	*Control of Procurements*
QA-NSLW-0501	*QA Implementing Procedures*
QA-NSLW-0601	*Document Preparation and Change*
QA-NSLW-0602	*Document Control*
QA-NSLW-0603	*Independent Technical Review*
QA-NSLW-0801	*Item Identification and Sample Control*
QA-NSLW-0901	*Special Processes*
QA-NSLW-1001	*Inspections*
QA-NSLW-1102	*Scientific Investigation for Applied Research*
QA-NSLW-1104	*Test Plans*
QA-NSLW-1106	*Operating Procedures*
QA-NSLW-1107	*Test Instructions*
QA-NSLW-1108	*Data Entry and Data Review*
QA-NSLW-1109	*Reporting*
QA-NSLW-1110	*General Documents*
QA-NSLW-1201	*Calibration and Control of M&TE*
QA-NSLW-1301	*Handling and Storage*
QA-NSLW-1401	*Status and Tagging*
QA-NSLW-1501	*Nonconformances*
QA-NSLW-1502	*Deficiency Reporting*
QA-NSLW-1601	*Significant Quality Issues*
QA-NSLW-1602	*Trending*
QA-NSLW-1701	*Record System*
QA-NSLW-1801	*Project Audits*

4.0 Materials and Methods

This section provides the details regarding the test approach, test equipment, and simulant material properties and preparation. The test approach and its associated limitations are described in Section 4.1. The test apparatus and associated equipment and instrumentation for implementing gas generation and release testing are described in Section 4.2. Simulant preparation steps and final test simulant properties (namely solids content, shear strength, and flow curve behavior) are described in Section 4.3. A complete list of bubble tests supporting this report is provided in Section 4.4.

4.1 Technical Approach

Current tests concern evaluation of gas release from simulants. However, to satisfy the overall DSGREP objectives outlined TP-DSGREP-013[1], experimental design efforts leading up to simulant testing also had to consider the feasibility of implementing the test method in remote, radiological environments such as hot-cells. Development of such methods reduces the entry cost for future gas release testing of actual Hanford wastes. Use of these same methods in the current study allows assessment of their performance against non-radiological test methods and provides a set of measurements against which actual wastes collected using hot-cell techniques can be compared. Experimental design efforts and any associated scoping tests are not documented in this report. However, a discussion of gas generation and release methods is given in this section to provide a rationale for the final experimental test method and apparatus selections presented in Section 4.2.

For gas generation and release morphology testing, experimental design focused on developing a method for gas generation and release testing that could be implemented in a radiological hot-cell environment (where equipment is remotely handled) and that would allow repeat gas generation and release testing on a limited waste sample inventory (250 to 500 mL). Of particular concern was the method used to generate a given volume of gas within the test material. Testing of gas retention and release has used several approaches for gas generation:

- addition of peroxide (e.g., Rassat et al. 2013; Gauglitz et al. 2013)
- addition of water-reactive metal powders such as iron or magnesium (Gauglitz et al. 2012; Powell et al. 2014)
- radiolysis of water and organics using an external high-dose radiation source (e.g., Gauglitz et al. 1996)
- nucleation and expansion of soluble gas under vacuum (e.g., Rassat and Gauglitz 1995)
- hydrophobic particle captive bubble expansion (e.g., Crawford et al. 2013)

The gas generation approach selected for cold simulant gas-release testing was nucleation and expansion of soluble gas under vacuum. In addition, several confirmatory tests support cold simulant testing employed addition of peroxide. Captive bubble expansion through addition of hydrophobic particles was identified as the suitable gas generation mechanism should future testing activities require

[1] Daniel R. 2013. Test Plan TP-DSGREP-013, Rev. 0.0 (or current revision). *Gas Release Testing in AY-102 Sludge*. Pacific Northwest National Laboratory, Richland, Washington.

implementation of gas-release tests in a hot-cell environment. The selection process is discussed briefly in Section 4.1.1. Vibration release of bubbles was explored as a physical mechanism for gas release study, using a small shaker table (see Section 4.1.2 for details). Other considerations, such as the applicability of vacuum testing relative to other release methods, are discussed in Section 4.1.3.

4.1.1 Gas Generation Methods

- **Addition of Peroxide / Reactive Metals**: Addition of peroxide or water-reactive metal powders is frequently used to generate bubbles in non-radiological physical simulant testing. Both peroxide and metal powders react with the test material or suspending phase to produce either hydrogen or oxygen gas. For hot-cell gas release testing, addition of reactive materials was avoided because both the reaction rate and extent are strongly material-dependent. When peroxide and iron are used for non-radiological gas release testing, scoping studies are often needed to determine the optimum concentration of reactive agent in a given test material to produce the desired fraction of gas. The vast majority of gas release testing employing peroxide and iron at PNNL to date has used a simple physical simulant (e.g., single solid minerals in water). Hanford wastes are complex chemical waste, involving a broad range of solid minerals and a suspending phase with a diverse range of concentrated electrolytes. Application of chemical gas generation techniques in wastes will be challenged by the range of potential chemical interactions between waste solids (both dissolved and insoluble) and hydrogen peroxide or iron. Such interactions could either accelerate or greatly hinder reactivity of gas-generating agents. For high-pH slurries, like Hanford tank waste, previous scoping tests indicated that hydrogen peroxide reacts quickly in high-pH waste materials. Likewise, reactive metals such as iron are expected to passivate under high-pH conditions and not react. For these reasons, use of reactive metals and/or peroxide solutions was avoided when considering gas generation methods for the current studies.

  Still, since peroxide addition was used both in the kaolin/bentonite slurry scoping tests providing the motivation for the current study (see Section 1.0) and in RT instability tests (Rassat et al. 2013), several confirmatory bubble generation and release tests that use hydrogen peroxide as a bubble source were performed under the current study.

- **Radiolysis of Water Using a High-Dose Source**: Hydrogen gas can be generated through radiolysis of water and decomposition of organics in the waste sample by placing the test material in contact with (or nearby) a high-dose radiation source. The process is akin to the same processes that generate hydrogen gas in the Hanford tanks, and is therefore highly applicable when testing with waste materials. Since actual waste samples typically must be handled in a remote shielded facility in the quantities needed for testing, the former requirement does not significantly impact the cost associated with testing of waste materials. To make radiolysis feasible for hot-cell testing, its occurrence is accelerated using a high-dose source. Gas generation testing in actual wastes conducted in the 1990s (see Gauglitz et al. 1996) used a high-dose 500 Ci ^{137}Cs source placed near the test sludge for several weeks. Hydrogen gas generated by proximity to the high-dose source was then expanded to the target volume fraction of gas by applying a vacuum to the test sludge. Use of a high-dose source is an advantageous means of gas generation, as it provides the same (albeit accelerated) gas generation mechanism found in Hanford tanks and can be used to generate gas on the same waste sample with minimal impact to chemistry. The main disadvantages of using a high-dose source are that exposure of samples to high-dose sources must be conducted in a shielded facility to minimize dose uptake by staff, it and requires significant exposure time (several weeks) to generate sufficient gas for a single

generation and release test. While no additional handling costs are incurred when testing radiological wastes, it does limit or greatly increase the cost of testing non-radiological simulants, especially if those simulants need to be disposed of as radiological waste as a result of handling in hot-cell environments (which are considered radiologically contaminated as a result of work with actual wastes and spent fuel samples). Despite this limitation, radiolysis by a high-dose source was considered the leading candidate for generation of gas in hot cell environments. It was eliminated because the cost of obtaining a high-dose source (~$250,000) equivalent to those used in previous studies was prohibitive and because of the need to implement radiological contamination and dose mitigation controls even when testing with cold simulants.

- **Nucleation and Expansion of Soluble Gases under Vacuum**: This approach uses gas that either is or can be dissolved into the test material to form nucleation sites for gas bubble generation and expansion under vacuum. For test slurries that already contain dissolved gas (such as atmospheric CO_2, O_2, or N_2), application of vacuum will cause this gas to come out of solution and expand within the test material. Likewise, soluble gases can be introduced into the test material by application of high-pressure soluble gas headspace over the test material, sparging of the test material with the soluble gas, or high-shear mixing of the test material in contact with soluble gas. Previous studies by Rassat and Gauglitz (1995) examined the use of NH_3 gas for bubble generation in actual wastes. Once dissolved, this gas can then be drawn out of solution by application of vacuum. Once bubble sites are nucleated, their size (and the fraction of gas within the test slurry) can be controlled by reducing or increasing the applied vacuum pressure. However, if too strong a vacuum is applied, it is possible to boil the suspending phase (typically water) and alter the composition of the test material. As typical gas release experiments aim to evaluate concentrated sludges at fixed (and well-known) solids concentrations, boiling is avoided as it could increase solids concentration and, as a result, material strength. The primary concern when using soluble gases is that dissolution or solubilization of the selected gas may impact the chemistry of the test material. For example, use of NH_3 gas in simulant materials prepared in suspending phases with intermediate pH and limited buffering capacity could drastically increase suspending phase pH and, as a result, alter the material strength during testing.

  Nucleation of naturally occurring gases in the test material (i.e., those resulting from exposure of the test sludge to atmosphere) was selected as the primary mechanism for gas release testing. Application of a vacuum will strip the test material of dissolved gases and limit the volume of gas produced when vacuum is applied to the same material in replicate tests. To overcome this limitation, dissolved gas was replenished by high-shear mixing.

- **Hydrophobic Particle Captive Bubble Expansion:** In this method, fine (10 to 100 μm) hydrophobic particles are slurried (at 0.1 to 1 vol%) into the test material. The hydrophobic particles are not fully wetted by the suspending phase and, as such, carry small pockets of entrained air into the test material. Subsequent sparging of the test slurry with air increases gas capture and hold-up by the hydrophobic particles. Upon application of a vacuum to the test mixture, captive bubbles will serve as nucleation sites for dissolved gases and will also expand to generate large bubbles, even in mixtures where the dissolved gas content is low. Gas capture by hydrophobic particles has been studied in the literature (Bryan et al. 1992; Zhou and Zhenghe-Finch 1998), and specific gas generation techniques using hydrophobic particle captive bubble expansion were developed for DSGREP gas generation and release morphology testing by Crawford et al. (2013). Hydrophobic captive bubble expansion was identified as the suitable gas generation mechanism should future

testing activities require implementation of gas-release tests in a hot-cell environment. For non-radiological simulant testing, it was rejected in favor of soluble gas nucleation techniques.

4.1.2 Gas Release

Release of retained gases from settled sludge in tanks, termed "gas release events," can occur through several mechanisms. A network of cracks and slits can form within the sludge as a result of gas generation and expansion, and subsequent breakthrough of those cracks and slits to the surface can effect a slow and continuous release. Release can occur without breakthrough of cracks to the surface. For example, if bubbles or pockets of gas grow sufficiently large, then their buoyant force can overcome the sludge yield stress, allowing the gas to rise through the sludge to the surface. Shearing of the sludge as the bubble/pocket rises can also effect release of adjacent bubbles, which can ultimately propagate the release event throughout the tank volume and lead to near complete release of gas from the tank. Such releases are called "bubble cascade gas release events."

Gas generation and release morphology testing is not concerned with the stability of gas generated within layers. Instead, it is concerned solely with the morphology of that gas release when the simulant is sheared. For this reason, all gas release events will be forced. The kaolin and bentonite studies that provided the motivation for the current work forced release by stirring the test materials with a flat spatula. However, because the primary means of gas generation testing for gas generation and release morphology testing involves application of a vacuum, the test dispersion cannot be accessed for direct mechanical agitation without breaking the vacuum and collapsing the entrained gas bubbles upon re-pressurization. Although direct mechanical agitation could be achieved through a magnetic stirrer, the efficacy of mixing and size of the disruption zone for standard magnetic stirring equipment would be limited in 30 Pa slurries. Likewise, a stir shaft could be coupled to an external mixer using a mechanical bearing seal. This seal could serve as a point of failure for the vacuum during testing. Instead, gas release for gas generation and release morphology testing was accomplished by vibrating the container holding the test material using a small vibrating table (see Section 4.2). Vibrating tables remove entrained gases by applying a relatively high-frequency (~50 Hz) but small-amplitude (~1 mm) oscillation to the test mixture. The vibrating tables' function is similar to, but much weaker than, sonic horns. Use of a vibrating table provides a simple means of effecting gas release from slurries in sealed test containers.

4.1.3 Other Considerations

The gas generation and release mechanisms selected for the main course of testing differ from those used in DSGREP companion studies (Rassat et al. 2013; Powell et al. 2014). For the majority of testing, gas nucleation is effected by application of vacuum as opposed to addition of hydrogen peroxide (or reactive metals), and gas release is effected by vibration as opposed to direct stirring or motion caused by a Rayleigh-Taylor instability. Given that use of a vacuum and vibration is a departure from gas generation and release methods typically used in DSGREP testing, this study also included several confirmatory gas generation tests, using the current test apparatus and instrumentation and using hydrogen peroxide as the gas source.

Application of a vacuum is not expected to appreciably affect gas release proclivity or morphology. Buoyant release of individual gas bubbles from a yield stress fluid is determined by the gravity-yield parameter *Y*, which is given by

$$Y = \frac{\tau_o}{(\rho_f - \rho_b) g d_b} \tag{4.1}$$

Here, an isolated gas bubble of diameter and density d_b and ρ_b, respectively, will rise through a fluid of yield stress τ_o and density ρ_f when *Y* falls below a critical-gravity yield parameter Y_C ranging from 0.061 to 0.088 (Laxton and Berg 2005). In this equation, *g* is the gravitational acceleration constant (9.81 m s^{-2}). For a bubble of given size, only the bubble density will be impacted by the test material headspace pressure. For all simulants considered herein (and in the DSGREP), the bubble (gas) density (~1 kg m^{-3}) is several orders of magnitude lower than the fluid density (~1000 kg m^{-3}). As such, the gravity-yield criterion is well approximated by

$$Y = \frac{\tau_o}{\rho_f g d_b} \tag{4.2}$$

and does not contain any terms impacted by headspace pressure. Therefore, the proclivity for bubble release without vibration or mechanical agitation should be similar for experiments conducted at atmospheric pressure and under vacuum. Under mechanical agitation, the rate of release is expected to be a function of both the forced flow field and bubble buoyancy. The flow field should be independent of pressure. Similar to the gravity-yield parameter, buoyancy depends on the difference in test material and bubble densities, and as a result, will be virtually independent of headspace pressure.

During release events, bubbles will rise through the test material and will be subject to decreasing hydrostatic pressure. The change in pressure acting on the bubble could allow for bubble growth (assuming the bubble pressure is sufficient to overcome the yield stress). Treating the bubble as an ideal gas, the maximum possible growth that could occur as a bubble rises from a depth of h_o in the test material[1] is described by the ratio *R* of the burst diameter d_e (i.e., that of the bubble as it reaches the surface) to its original diameter d_o at depth h_o:

$$R = \frac{d_e}{d_o} = \left(1 + \frac{\rho g h_o}{P_h}\right)^{1/3} \tag{4.3}$$

Here, ρ is the density of the fluid controlling bubble pressure (either that of the suspending phase or the bulk density of the test slurry), and P_h is the headspace pressure. It should be noted that Eq. (4.3) assumes that bubble growth during rise occurs at a constant temperature. Equation (4.3) demonstrates that bubble growth can become significant when the change in bubble pressure ($\rho g h_o$) is greater than or of similar magnitude to the headspace pressure. As such, potential bubble growth is of concern when testing under vacuum. As discussed in Section 4.4, the DSGREP test column will typically be filled with

[1] Here, and for the expression that follows, the test depth h_o corresponds to that of a negligibly small bubble in an otherwise gas-free material. This approach provides a good measure of the impact of hydrostatic pressure on bubble size while avoiding the complexity of predicting/modeling hydrostatic and bubble pressure in non-uniform, bubble-laden slurries.

10 cm of test simulant with densities no greater than 1250 kg m^{-3}. Bubble rise under atmospheric headspace conditions will see bubble ratios no larger than 1.004 (e.g., bubbles will grow by no more than 0.4%). At the lowest pressures tested herein (~50 torr), the bubble growth ratio will be no larger than 1.06 (e.g., bubbles will grow by no more than 6%). In practical terms, this means that a 5.0 mm bubble released from the bottom of the test container will grow no larger than 5.3 mm when it bursts at the surface. In terms of gas release morphology, this increase will be undetectable with the imaging system used to record gas release.

Given the considerations discussed above, it is reasonable to postulate that use of a vacuum to grow nucleated bubbles in the current studies will not appreciably affect the gas release morphology relative to studies conducted at atmospheric pressure. This is not to say that the different mechanism used for producing bubbles (i.e., dissolved gas nucleation versus decomposition/reaction of peroxide) will produce the equivalent bubble count and size distribution within the test matrix. However, the bubble size distribution has not been explicitly considered or measured in any DSGREP simulant testing to date. The current testing did not attempt to quantify or match bubble size distribution generated by application of vacuum to that generated by peroxide reaction. Furthermore, no attempt was made to match or infer bubble size distribution across simulants.

4.2 Apparatus and Instrumentation

Figure 4.1 shows a simplified schematic of the primary bubble test apparatus and setup used in gas generation and release morphology testing. The test apparatus consists of an acrylic graduated cylinder with a 5 cm diameter and a total height of 25 cm. The test column has a 15 cm circular acrylic base (1 cm in height) and a stainless steel sanitary fitting adaptor at the top. Graduations mark 0.5 cm intervals along the vertical height of the column. The column lid is attached to the column using a sanitary clamp and a Teflon O-ring. To create a secure seal that would prevent loss of vacuum over time during testing, the O-ring is lubricated with high-vacuum grease. The column lid is made of acrylic and contains an attachment port to connect the column to vacuum. During testing, the column rests freely upon a shaker table, specifically a Whip Mix General Purpose Vibrator (Item No. 10650). It is estimated that the shaker table provides vibration amplitudes of ~1 mm (±0.5 mm) at frequencies of ~50 Hz.

The vacuum side of the test apparatus contains two on/off ball valves (valve #1 and valve #2), a variable needle valve (valve #3), a high-efficiency particulate air (HEPA) filter, and vacuum gage. Valve #1 (a ball valve) is the column "vent" and allows the column to be quickly re-pressurized after testing. It is closed under normal column operation. The HEPA filter prevents any fine particulate and aerosols from being pulled into the building vacuum system that provides vacuum for testing. Valve #2 (a ball valve) allows the column to be isolated from the vacuum system. It is normally open when vacuum is being drawn on the test simulant. Once the desired vacuum is achieved, valve #2 is closed, and the bubble release is conducted in the isolated system. The vacuum pressure is monitored by a vacuum transducer coupled to a digital display. The transducer and display are a Varian Model 6543-25-015 (SN# 20725002) and Model 6522-08-410 (SN# 20724004), respectively. Both transducer and display have been calibrated as a unit (PNNL barcode ID #20686) to measure pressure over 10 to 500 torr to within ±2% of reading or ±2 torr (whichever is greater). Valve #3 (a needle valve) allows adjustment of the vacuum pressure and functions by allowing bypass air into the vacuum system. During testing, it is either 1) closed to achieve full building vacuum or 2) set to achieve a rough vacuum (200 to 300 torr) and subsequently adjusted downward until the desired test conditions (either a target vacuum pressure or gas

expansion) are achieved. The vacuum side of the test apparatus is connected to building vacuum in PNNL's Life Science Laboratory 2 (LSL2). The building vacuum provides 50 ± 2 torr.

Several secondary confirmation tests used hydrogen peroxide to generate bubbles. These additional confirmatory tests used standard laboratory glassware, including a standard 2 L beaker and 100 mL graduated cylinder.

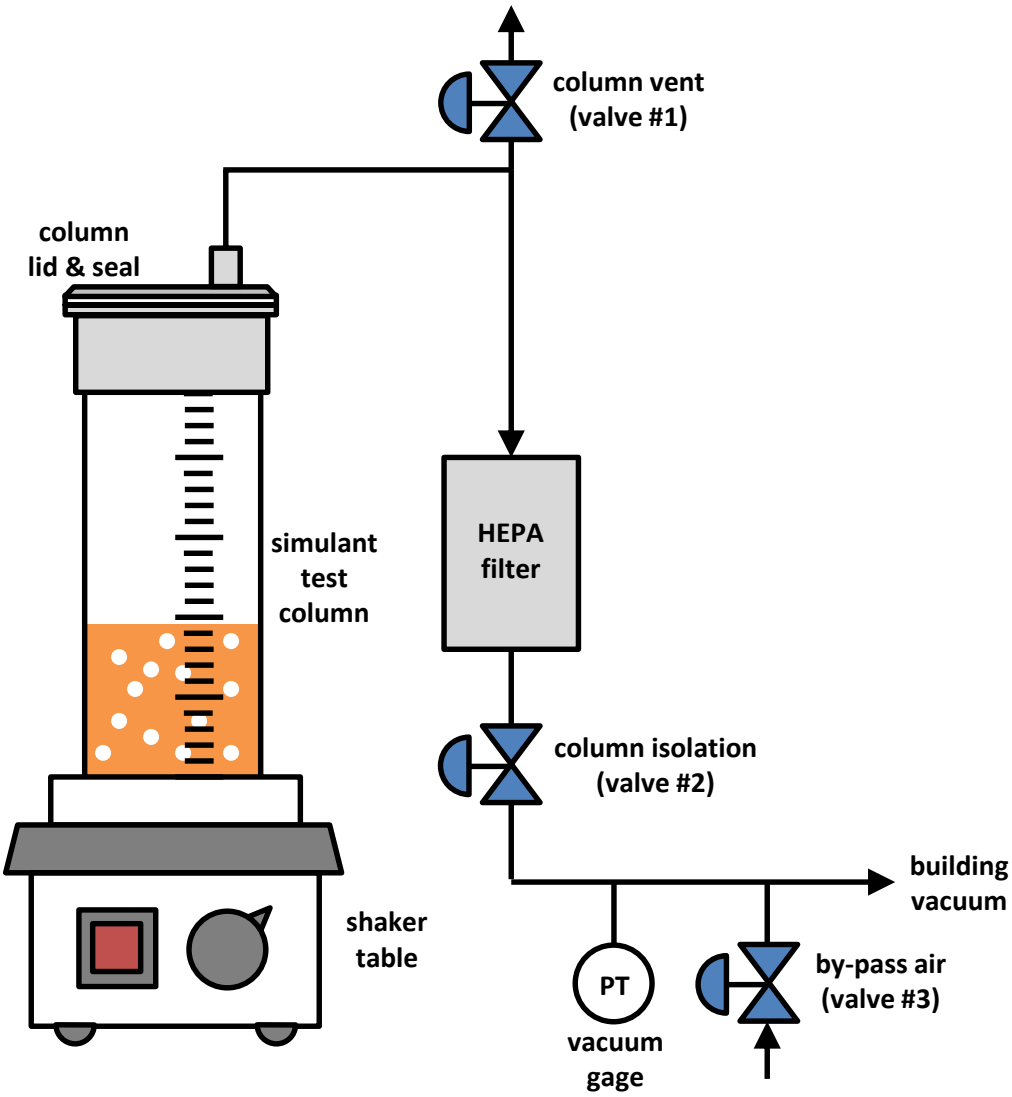

Figure 4.1. Bubble Generation and Release Test Setup (not-to-scale)

4.3 Simulants

The revised scope for gas generation and release morphology testing called for the evaluation of three simulant materials: a 30 Pa kaolin clay slurry, a 30 Pa bentonite clay slurry, and a 30 Pa RT Simulant slurry. For all material, the "30 Pa" designation refers to the target value of shear strength taken 1 hour after the material was last mixed thoroughly. Bentonite and kaolin clay slurries are simple mixtures of

dry bentonite and kaolin powder mixed in Richland city water (RCW). The RT Simulant is a dry powder mixture of 90 wt% Min-U-Sil 30 (silica) and 10 wt% bentonite slurried in RCW and pH adjusted to 4.4 using 6 M hydrochloric acid. The composition, shear strength, and rheology of the final prepared simulants were evaluated before testing. The following sections discuss the simulant preparation and physical characterization methods and test results.

Table 4.1. Simulant Bulk Materials Identification List

Simulant Name	Simulant Composition	Manufacturer	Product ID
Bentonite	Bentonite/RCW[(a)]	Wyo-Ben, Inc.	Big Horn® BH 200
Kaolin	Kaolin/RCW	Edgar Minerals	EPK, clay
RT Simulant	Bentonite/Ground Silica/RCW	U.S. Silica	Min-U-Sil® 30

(a) RCW is Richland city water.

4.3.1 Simulant Preparation

The bulk materials used for simulant preparation are identified in Table 4.1. Scoping tests were performed to identify the ratio of dry solids to RCW needed to produce the target rheology of 30 Pa for each of the three simulants. To create the kaolin and bentonite slurries, the dry clay powders referenced in Table 4.1 were slurried in water, shaken by hand, and then sheared for at least 1 minute in a Magic Bullet blender purchased from Homeland Housewares®. To prepare the RT Simulant, a batch of dry-mixed 90:10 Min-U-Sil 30:bentonite powders was prepared by weighing the individual dry components into a bottle and rolling the bottle to dry-mix the solids. After dry-mixing, the solid components were blended with water using a Magic Bullet until a homogenous mixture was obtained. Once mixed, the initial RT Simulant slurry was allowed to rest for 4 hours and then pH adjusted to 4.4 using 6 M HCl solution. Twenty-four hours after initial pH adjustment, the pH was retested and, if needed, readjusted to 4.4 using 6 M HCl solution.

For the primary course of testing described in this report, bubble generation relied entirely on dissolved gas content. For these tests, simulants could be made to their target strengths (as described above) and used directly. In addition to the standard tests, there were several confirmation tests that employed hydrogen peroxide to generate bubbles for gas release testing. In these tests, a dilute 3% hydrogen peroxide solution in water was mixed with the simulant materials. Simulant recipes were adjusted such that the simulants were initially prepared with the solid powders and RCW. No hydrogen peroxide was added initially, but the simulants were prepared at higher solids concentrations to accommodate addition of 3% hydrogen peroxide solution at the start of testing. Initial slurry concentrations were selected based on the target hydrogen peroxide concentrations (see Table 4.2) and the expected strength after dilution. The simulant slurries, without hydrogen peroxide, were allowed to age for at least 24 hours (to fully hydrate the simulant solids and avoid rapid changes in shear strength associated with solid hydration) and, in the case of RT Simulant, adjusted to the target pH with 6 M HCl solution. Once the simulant was fully aged and ready for testing, 3% hydrogen peroxide solution (Ricca Chemical Company, Arlington, Texas) was added to achieve the target peroxide concentration. All target peroxide concentrations were selected to yield 15 vol% entrained gas after 16 hours of peroxide decomposition and bubble growth.

Once the simulant slurries were prepared, subsamples were taken for physical characterization, namely shear strength measurement. Bubble generation and release tests were only conducted on a given simulant material if the shear strength, measured 1 hour after mixing of the simulant material, fell between 15 and 45 Pa. A shear strength of 30 Pa 1 hour after mixing was targeted for all simulants. If the material fell outside this range, the solids concentration was adjusted either by addition of dry solids or dilution with RCW. The simulant was then remixed and its shear strength tested again for acceptance.

Table 4.2. Target Hydrogen Peroxide Concentrations for Hydrogen Peroxide Bubble Generation in Gas Generation and Release Morphology Testing Simulants

Simulant	Target Hydrogen Peroxide Concentration (gram H_2O_2 / 100 gram slurry)
30 Pa bentonite clay	0.045
30 Pa kaolin clay	0.36
30 Pa RT Simulant	0.10

4.3.2 Laboratory Measurements

The following analytical techniques were used to characterize the simulant materials prepared for gas generation and release morphology testing:

- pH
- shear strength
- flow curve
- solids content
- mass
- temperature
- video

Not all physical properties were characterized for every simulant. Notably, pH was only measured for the RT Simulant because preparation of this simulant required pH adjustment. The current section only discusses measurement methods. Section 5.1 summarizes measured simulant physical properties.

- **pH:** The pH of the RT Simulant was measured using an Accumet AP85 meter coupled with an Accumet pH probe (model 13-620-AP55). The Accumet meter displays pH to a resolution of ±0.01. pH adjustments of the RT Simulant were made to an accuracy of ±0.1. RT Simulant pH is not reported in this document.
- **Shear Strength:** Shear strength represents the force required to initiate motion in a bed of settled solids. Shear strength measurements were performed using a Haake RS600 rheometer coupled with an FL22 vane tool (a four-paddled vane with nominal dimensions of 22 mm wide by 16 mm high). Measurements were made at ambient laboratory temperature in accordance with PNNL procedure

RPL-COLLOID-02, Rev. 2.[1] Measurements were made immediately following mixing, after 1 hour of gelation, and (for the hydrogen peroxide test simulants only) after 16 hours of gelation. Mixing involved vigorous hand-shaking of the samples for approximately 30 seconds.

- **Flow Curve:** Flow curve measurements map the stress response of a fluid as a function of shear rate. Flow curves can be used to determine material flow characteristics, such as fluid yield stress and consistency and apparent viscosity. Flow curves for each of the simulant materials were measured using an RS600 rheometer coupled with a Z41 concentric cylinder measuring geometry. Measurements were made at 25 °C in accordance with PNNL procedure RPL-COLLOID-02, Rev. 2. For flow curve measurements, temperature was controlled by a Haake Fisons F3/CH recirculating water bath. Flow curve measurements consisted of three periods of rotation: 1) an up-ramp period where the shear rate was gradually increased from 0 to 1000 s^{-1} over 5 minutes, 2) a 1-minute period of constant rotation at 1000 s^{-1}, and 3) a down-ramp period where the shear rate was gradually reduced from 1000 to 0 s^{-1}. Each flow curve measurement was preceded by a 3-minute-long pre-shear of the material at 200 s^{-1}. Flow curves (i.e., the shear stress versus shear rate response curves) are characterized using a Bingham-Plastic model, such that

$$\tau = \tau_{B,o} + K_B \dot{\gamma} \tag{4.4}$$

  Here, τ is shear stress and $\dot{\gamma}$ is the shear rate. A Bingham-Plastic fluid is characterized by two flow parameters: 1) $\tau_{B,o}$ is the yield stress and represents the minimum force needed for viscous flow, and 2) K_B is the consistency and represents the slope of the stress-rate response curve. Values of Bingham-Plastic consistency and yield stress are determined by application of linear regression to the measured shear stress – shear rate response.

- **Solids Content:** The solids content (i.e., the weight percent solids) of each simulant material was measured for informational purposes. For the current testing, solids content does not have any direct bearing on the test measurements other than to confirm simulant preparation (by comparing the actual solids concentration to that expected from material balance) and to indicate anomalous simulant behavior (e.g., a sample that meets rheology targets but has a lower-than-expected solids content). The solids content of the simulants was measured using a Mettler-Toledo HR83 Moisture Analyzer.

- **Mass:** Preparation of simulants required careful weighing of solid and liquid components. Component masses were weighed using one of two balances: a Mettler Delta Range XA204 or a Sartorius BP3100S. The Mettler Delta Range XA204 is a four-place balance with an upper measuring range of 220 g. The Sartorius BP3100S is a two-place balance with an upper range of 3100 g. Simulant masses are not reported in this document.

- **Temperature:** Temperature was measured using an Omega Type-K thermocouple coupled with an Omega model MDSSi8 temperature display. The temperature display and thermocouple are calibrated separately over a range of 0 to 100 °C (PNNL barcodes 22890 and 38617, respectively). Each unit has an associated uncertainty of ±2.0 °C. Laboratory and sample temperatures are not reported in this document.

[1] Daniel R. 2010. *Measurement of Physical and Rheological Properties of Solutions, Slurries and Sludges.* RPL-COLLOID-02, Rev. 2. Pacific Northwest National Laboratory, Richland, Washington.

- **Video:** Gas generation and release testing was captured on a high-definition video recorder. Simulant heights were measured from the video images by using the graduation marks on the test cylinder. For all test approaches, video capture provided a visual record by which the gas release morphology could be evaluated. The graduations on the test cylinder provided a means of judging change in slurry level (or volume) and also provided a scale against which semi-quantitative evaluations of bubble size could be made. The standard test column described in Section 4.1 provides slurry height graduations. Measurements of slurry level recorded by video could be used to calculate the fraction of slurry volume occupied by gas. The fraction of gas contained in a slurry (denoted as X) was calculated by comparing slurry level H (i.e., that after generation of gas) to the initial slurry level H_o (i.e., that before generation of gas):

$$X = \frac{H - H_o}{H} \tag{4.5}$$

  The 2 L beaker and 100 mL graduated cylinder used in confirmatory testing provide volume graduations. When testing in these vessels, the gas fraction was calculated from the current slurry volume (with gas) V and the initial gas free volume V_o:

$$X = \frac{V - V_o}{V} \tag{4.6}$$

  Initial column level or volume was recorded immediately after loading the test material into the test container. Target bubble growth conditions (e.g., 15 vol%) were achieved by monitoring the change in level during the growth period. During release of gas from the test containers, the change in level was continuously monitored by video capture. Video was captured at a rate of 24 frames per second. When analyzing the video feed, images were evaluated at intervals that range from 1 to 10 seconds (depending on the rate of gas release from the simulant).

  For testing in the primary test apparatus and the 100 mL graduated cylinder, side views of the test column and simulant were captured (e.g., see Figure 5.3). During 2 L beaker stir tests, the surface of the test simulant was monitored using a top-down view. This prevented assessment of slurry level during gas release. Instead, the pre- and post- release slurry levels were recorded.

4.4 Test Approach and Matrix

All three simulant mixtures were subjected to bubble generation and release testing using the apparatus described in Section 4.2. Prior to gas generation and release testing, the column was vacuum tested to verify that the system was “air-tight.” Verification was performed by sealing and evacuating the test column (with the vent and vacuum by-pass valves closed) to the maximum building vacuum of 50 torr. The building vacuum valve (not shown in Figure 4.1) was closed and the vacuum pressure monitored as a function of time. If the vacuum pressure did not increase by more than 10 torr over a 2-minute period, then the column seal was considered acceptable. If the column was unable to meet this vacuum test requirement, corrective action was taken and generally involved verifying the tightness of Swagelok fittings on the vacuum line and applying high-vacuum grease to the column lid and seal.

Primary gas generation and release testing of simulants, which used the test apparatus shown in Figure 4.1, consisted of seven steps:

1. verification of the simulant shear strength
2. loading of the column with simulant
3. controlled evacuation of the column headspace, leading to bubble generation and expansion
4. isolation of the column and verification that vacuum pressure is held
5. application of vibration to release bubbles
6. release of vacuum
7. test column clean-out

The first step in testing was to verify that the shear strength of the test material was acceptable. A shear strength of 30 Pa (after a gelling period of 1 hour) was targeted for all simulants; however, the strength of the material was considered acceptable for testing if it fell within 15 to 45 Pa after 1 hour of gelation. If the test material failed to meet the targeted strength, then its concentration was adjusted (as needed) or the simulant was prepared a second time from the starting materials.

Once the target strength was achieved, the simulant material was loaded into the column to a target height of 10 cm. This test height corresponds to approximately 200 mL of material. After loading, the column was sealed and evacuated by closing the column vent valve (valve #1) and opening the building vacuum valve and column isolation valve (valve #2). Initial gas generation and release testing was performed at maximum building vacuum (50 torr). Here, the vacuum by-pass valve (valve #3) was closed during evacuation, such that the maximum vacuum was achieved in the column. Application of full vacuum generally resulted in simulant gas fractions ranging from 20% to 30%. Gas generation and release testing was also performed at a constant gas volume of 15%. Here, initial evacuation was performed with the vacuum by-pass valve (valve #3) open. This limited the maximum vacuum generated to ~250 torr. The by-pass valve was then slowly closed until a fraction of 15% was achieved. Evacuation of the column and generation and expansion of bubbles thereafter were captured on video.

After the target pressure or gas fraction was achieved, the column was isolated by closing valve #2. The height of the expanded test simulant was monitored for 1 minute to verify the seal. Any decrease in slurry height (without a corresponding release of bubbles from the surface) was taken to indicate loss of vacuum pressure in the column. If a drop in the expanded simulant was observed, the test was stopped, corrective actions were taken to improve the column seal, and the test was repeated.

Next, vibration was applied to release the bubbles entrained in the test material. The column was gently placed on a shaker table and the shaker table activated. A vibration intensity[1] setting of 8 was used

[1] The vibration intensity is controlled by a dial on the vibrating table and has settings from 0 (lowest) to 10 (highest). Changing the vibration intensity setting appears to change the amplitude of vibration (rather than the frequency, which is around 50 Hz). No rigorous attempt was made to quantify the amplitude of vibration produced by the table. Estimates indicate that the highest amplitude setting appears to produce an oscillation no larger than ±0.5 mm. The vibration intensity used for the primary course of testing was determined through scoping tests, which identified the vibration setting that effected release of vacuum-generated bubbles over several minutes of testing.

for the entirety of gas release testing. The intensity of vibration was varied by applying downward force on the column (i.e., by holding it more tightly against the vibration table). Low-intensity was achieved by holding the column firmly against the shaker table surface, which limited the vibrational displacement of the column to that of the shaker table itself (with a total displacement amplitude no greater than 1 mm). High-intensity vibration was achieved by loosely holding the column against the shaker table, which allowed the column to bounce and achieve up to a 2 mm displacement. Scoping tests indicated that varied intensity was needed to reproducibly remove entrained gas from the test simulant. The intensity schedule was 15 seconds of low intensity vibration followed by 5 seconds of high intensity vibration. This schedule was repeated for up to 150 seconds of total vibration. During this time, gas bubbles would coalesce and rise to the surface of the test simulant. Release of gas would decrease the level of simulant recorded, by video, as a function of vibration and time. At the end of the vibration period, the vibrating table was turned off and the column level recorded while still under vacuum. Next, the column vacuum was released by opening the column vent valve (valve #1). Any change in level during release was captured by video.

At the end of testing, the test simulant was removed from the column and placed into a secondary container away from the primary simulant batch. Simulant hold-up on the walls was cleaned off and collected in the secondary container. The column was then rinsed and dried and readied for the next test. Dissolved gas in the spent simulant was regenerated by blending in a high-shear mixer. Subsequent column tests used either a fresh or a regenerated batch of simulant.

A matrix of 18 primary bubble generation and release tests were performed. As described above, testing employed two strategies: 1) gas generation at maximum vacuum (50 torr) and 2) gas generation at a variable pressure to achieve 15% gas volume. Within each pressure strategy, tests involved generation and release from three simulants (30 Pa kaolin clay, 30 Pa bentonite, and 30 Pa RT Simulant), with a primary test and two replicate tests performed for each simulant material. In addition to these 18 tests, nine confirmatory tests were also performed. These involved a single test of each simulant material, with gas generated by reaction/decomposition of hydrogen peroxide, performed in a 2 L beaker, in the primary test column shown in Figure 4.1, and in a 100 mL graduated cylinder (3 cm in diameter and 25 cm in height). All testing with hydrogen peroxide was conducted at atmospheric pressure. For vibration release testing in the primary test apparatus, a vibration table amplitude setting of 8 was used. For vibration release testing in the 100 mL graduated cylinder, a vibration table amplitude setting of 4 was used. For stir testing, gas release was effected by stirring with a 1-inch-wide, 6-inch-long metal spatula for 1 minute. Table 4.3 provides a matrix of all test performed in support of gas generation and release morphology testing.

Table 4.3. Matrix of Bubble Generation and Release Studies for Gas Generation and Release Morphology Testing

Simulant Material	Gas Generation Method	Test Vessel	No. of Tests
30 Pa bentonite	Vacuum (at 50 torr)	Sealed Test Column	3
	Vacuum (to 15% Gas Volume)	Sealed Test Column	3
	Hydrogen Peroxide	2 L Beaker	1
	Hydrogen Peroxide	Primary Test Column	1
	Hydrogen Peroxide	100 mL Graduated Cylinder	1
30 Pa kaolin	Vacuum (at 50 torr)	Sealed Test Column	3
	Vacuum (to 15% Gas Volume)	Sealed Test Column	3
	Hydrogen Peroxide	2 L Beaker	1
	Hydrogen Peroxide	Primary Test Column	1
	Hydrogen Peroxide	100 mL Graduated Cylinder	1
30 Pa RT Simulant	Vacuum (at 50 torr)	Sealed Test Column	3
	Vacuum (to 15% Gas Volume)	Sealed Test Column	3
	Hydrogen Peroxide	2 L Beaker	1
	Hydrogen Peroxide	Primary Test Column	1
	Hydrogen Peroxide	100 mL Graduated Cylinder	1
Total			27

5.0 Test Results

This section presents the results of gas generation and release morphology testing. Section 5.1 presents select physical properties of the three test simulants. Section 5.2 details the result of vacuum testing at 50 torr. Section 5.3 details gas generation tests performed at 15 vol% (with variable pressure). Section 5.4 presents the test results for hydrogen peroxide follow-on testing. A summary of gas generation and release results and concluding remarks is deferred to Section 6.0 of this report.

5.1 Test Simulant Properties

The three simulant materials—30 Pa bentonite clay, 30 Pa kaolin clay, and 30 Pa RT Simulant—were prepared to support the three separate gas generation and release tests, namely tests at constant vacuum pressure (50 torr), tests at constant gas volume (15 vol%), and tests using hydrogen peroxide. Table 5.1 lists the weight percent total solids for each test simulant for each of the three generation and release tests. In general, there is little test-to-test variation in the weight percent solids of the simulants. Table 5.2 presents the shear strengths of test slurries immediately following mixing and after 1 hour of gelation for each of the three gas generation and release tests. For testing with hydrogen peroxide, only the shear strength after 16 hours of gelation is reported, as this most closely represents the actual strength at release. For vacuum tests (both at constant pressure and constant gas volume), testing occurred shortly (~15 minutes) after the test material is mixed. As such, the shear strength immediately following mixing was most representative of the material strength at release. The material strength is gaged by the shear strength, as measured 1 hour after mixing. For all simulants, the shear strength fell within the acceptable test range of 15 to 45 Pa.

Table 5.1. Weight Percent Total Solids of Gas Generation and Release Test Simulants

Simulant	Test	Weight Percent Total Solids (%)[(a)]
30 Pa bentonite	Vacuum (at 50 torr)	8.5
	Vacuum (to 15% Gas Volume)	8.5
	Hydrogen Peroxide	8.3
30 Pa kaolin	Vacuum (at 50 torr)	33.5
	Vacuum (to 15% Gas Volume)	33.0
	Hydrogen Peroxide	33.6
30 Pa RT Simulant	Vacuum (at 50 torr)	48.1
	Vacuum (to 15% Gas Volume)	48.2
	Hydrogen Peroxide	48.4

(a) Weight percent total solids measurements have an associated uncertainty of ±0.1%.

Table 5.2. Shear Strength of Gas Generation and Release Test Simulants

Simulant	Test	Shear Strength[(a)] After Mixing (Pa)	Shear Strength After 1 hour (Pa)	Shear Strength After 16 hour (Pa)
30 Pa bentonite	Vacuum (at 50 torr)	17	23	n/a
	Vacuum (to 15% Gas Volume)	19	24	n/a
	Hydrogen Peroxide	n/a	n/a	22
30 Pa kaolin	Vacuum (at 50 torr)	24	26	n/a
	Vacuum (to 15% Gas Volume)	26	26	n/a
	Hydrogen Peroxide	n/a	n/a	36
30 Pa RT Simulant	Vacuum (at 50 torr)	15	23	n/a
	Vacuum (to 15% Gas Volume)	20	21	n/a
	Hydrogen Peroxide	n/a	n/a	38

(a) Shear strength measurements are accurate to ±1 Pa.

Table 5.3. Best-Fit Bingham-Plastic Parameters for Each Test Simulant[(a)]

Simulant	Yield Stress (Pa)	Consistency (mPa s)
30 Pa bentonite clay	15.5	16.4
30 Pa kaolin clay	57.5	17.2
30 Pa RT Simulant	12.4	18.1

(a) Yield stress and consistency results are determined by linear regression of the down-ramp over 200 to 1000 s^{-1}.

Figure 5.1A, Figure 5.1B, and Figure 5.1C show the flow curve (i.e., shear stress / shear rate response) of 30 Pa bentonite, 30 Pa kaolin, and 30 Pa RT Simulant, respectively. Prior to execution of the flow curve measurements shown, the test slurries were subjected to a sample pre-shear of 200 s^{-1} for 3 minutes. The solid curve in each figure shows the best fit of the flow behavior using a Bingham-Plastic model, Eq. (4.4), with the fitting region limited to 200 to 1000 s^{-1} on the down-ramp portion of the curve. The best-fit Bingham-Plastic parameters for all three simulants are presented in Table 5.3. In terms of the flow curve measurement themselves, a diverse range of flow behaviors is observed for the simulant materials tested. For 30 Pa bentonite, the Bingham-Plastic yield stress of 15.5 Pa is below that of the freshly mixed shear strength of 17 to 19 Pa. This is expected, given the pre-shear regimen applied to the flow curve sample. In addition, the up- and down-ramp curves for 30 Pa bentonite almost overlap each other, with the down-ramp falling just below the up-ramp. The behavior indicates a very slight thixotropy. The flow curve presented by 30 Pa kaolin clay is anomalous. The Bingham-Plastic yield stress is 57.5 Pa, and is much larger than the measured shear strength for this sample (24 and 26 Pa immediately after sample mixing). The flow curve suggests significant rheopecty. The anomalous Bingham-Plastic yield stress likely results from shear-induced thickening of the kaolin clay slurry during pre-shear and flow-curve measurements. For 30 Pa RT Simulant, the yield stress is 12.4 Pa and falls below the measured shear strength of 15 and 20 Pa. The flow curve indicates that RT Simulant is thixotropic; as such, the relatively low yield stress (relative to the measured shear strength) likely results from shearing of the test sample during the pre-shear and initial shearing steps in the flow curve measurement.

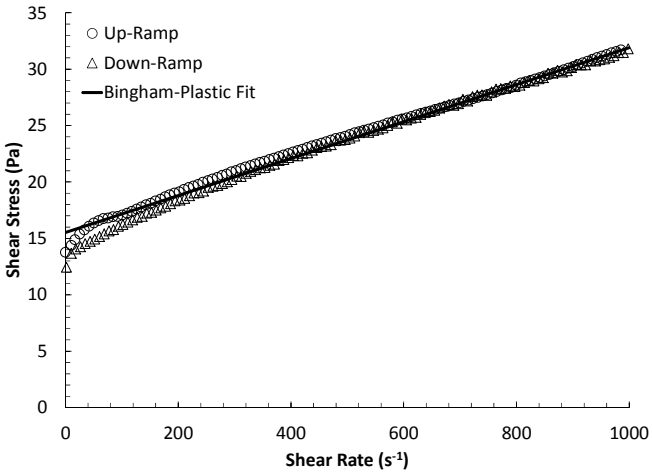

(A) – 30 Pa bentonite clay

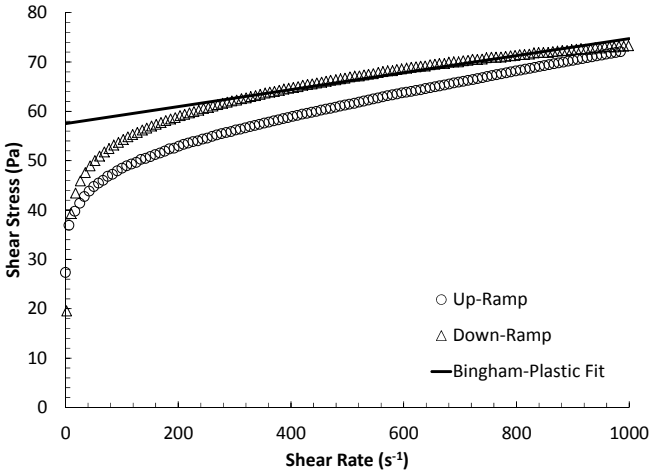

(B) – 30 Pa kaolin clay

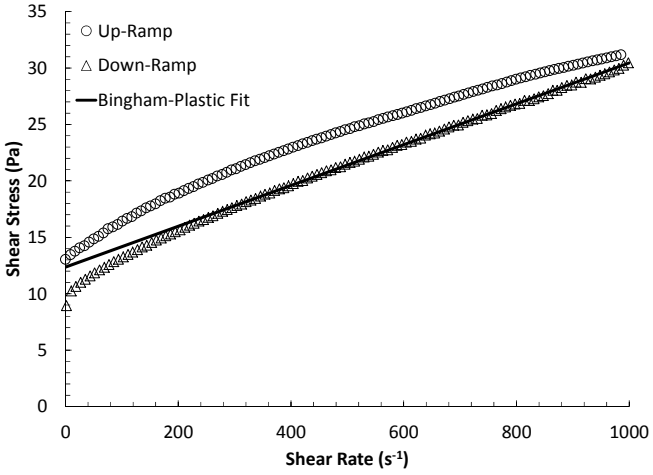

(C) – 30 Pa RT Simulant

Figure 5.1. Flow Curves for (A) 30 Pa Bentonite Clay, (B) 30 Pa Kaolin Clay, and (C) 30 Pa RT Simulant. Solid line represents best fit of the Bingham-Plastic model [Eq. (4.1)]. Fitting parameters are listed in Table 5.3.

5.2 Bubble Generation and Release at Constant Vacuum

Gas generation and release testing at constant pressure refers to tests where bubbles were generated at 50 torr vacuum pressure. In general, this produced entrained gas fractions greater than the target of 15 vol% and, because of differences in the dissolved gas content of each simulant material, also produced differences in entrained gas fraction from test-to-test and simulant-to-simulant. Despite the test-to-test variations and the fact that the entrained gas fraction is larger than desired, these tests provide useful gas release information.

Figure 5.2 shows the initial gas fraction generated at 50 torr in each of the three simulants and for each of the three tests (one primary and two replicates) for each simulant. Entrained gas fractions generated at 50 torr range from 18 to 24 vol% and are usually fully generated after 1 to 2 minutes of vacuum. Select images of the bubbles generated in 30 Pa bentonite, kaolin, and RT Simulant are given in Figure 5.3. In general, bubbles appear to be largest in the bentonite clay slurry and smallest in the kaolin clay slurry. No attempt was made to measure the bubble size distribution from those bubbles visible at the wall. The bubbles appear to be evenly distributed throughout the slurry in all test simulants.

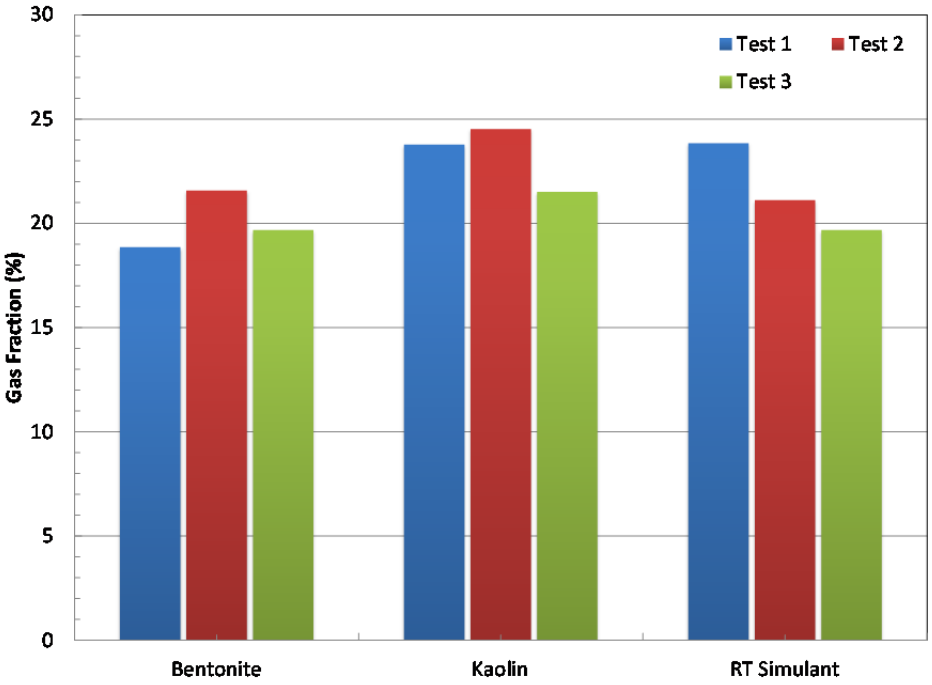

Figure 5.2. Entrained Gas Fraction Generated in Each 30 Pa Simulant at 50 torr Vacuum. Test 1 is the primary test, whereas Tests 2 and 3 are the replicate tests.

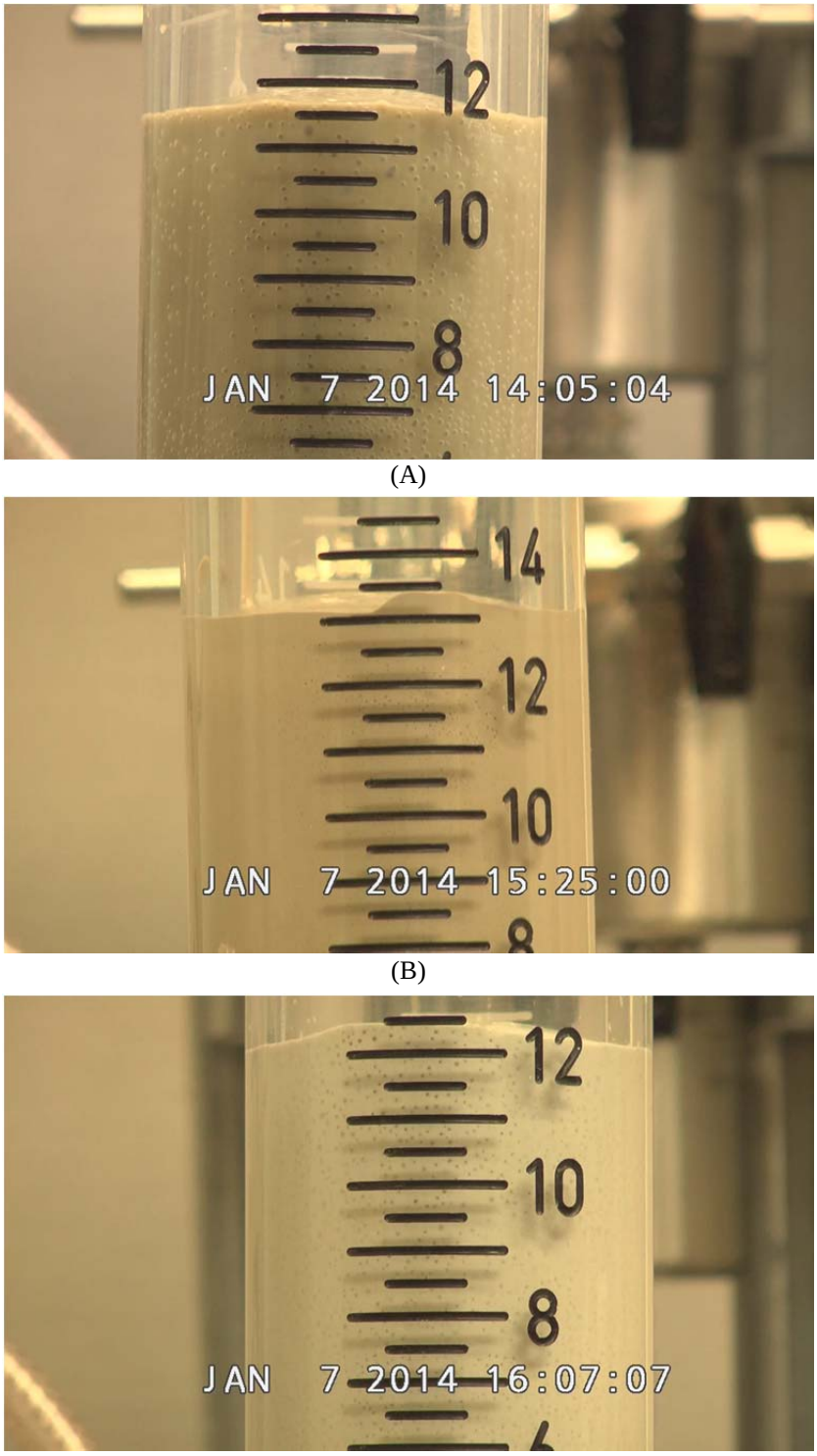

Figure 5.3. Select Images of Bubbles Generated at 50 torr Vacuum (bubble generation time ~1 minute) in (A) 30 Pa Bentonite Clay, (B) 30 Pa Kaolin Clay, and (C) 30 Pa RT Simulant. (Note: Column height is in centimeters.)

Figure 5.4 shows the gas release profiles for each simulant. The release behavior of each simulant appears to be unique, with some simulants showing only partial release and others showing rapid and complete release. For 30 Pa bentonite (Figure 5.4A), gas release primarily occurs within the first 40 seconds of vibration and corresponds to a drop in entrained gas volume from approximately 20% gas to 5% to 10% gas. After this initial release, further release of gas is minimal such that 5% to 10% gas is still entrained at the end of testing. Release of vacuum at the end of 30 Pa bentonite clay testing causes the remaining gas to collapse. Gas release from 30 Pa kaolin (Figure 5.4B) occurs slowly but reaches a near-complete release. Specifically, there is a slow but monotonic release of gas from kaolin in which the gas fraction decreases from its initial value of ~23% down to 1% to 2% after 100 seconds. Relative to the two clay simulants, gas release from 30 Pa RT Simulant (Figure 5.4C) occurs rapidly and completely, with the entire volume of entrained gas (~20%) being fully released after 50 seconds of vibration.

Figure 5.5 compares simulant gas release behaviors. Here, a normalized gas release profile has been generated by averaging primary and replicate test data for each simulant, and then by normalizing the gas fraction to the average initial fraction observed for all simulant tests (~21.7%). This treatment facilitates comparison of gas release behaviors across simulants. Figure 5.5 indicates that the gas release behavior from the 30 Pa kaolin and bentonite slurries is initially similar over the first 70 seconds. However, bentonite clay retains gas whereas kaolin clay does not. Release of gas from the RT Simulant occurs rapidly (relative to the two other test simulants) and is complete. Indeed, of all three test simulants, the RT Simulant shows the most rapid and complete release when tested at 50 torr.

The results shown in Figure 5.5 do not agree with expectations. The initial scoping tests providing the motivation for gas generation and release morphology testing indicated that the bentonite clay would release rapidly and completely while kaolin would retain gas. The results obtained at 50 torr vacuum using a shaker table are reverse of the expectations: bentonite clay retains gas whereas kaolin does not. There are several differences in the scoping and DSGREP bubble release tests that could cause the difference in gas release behaviors. First, bubbles are generated by vacuum in the current tests as opposed to peroxide in the scoping tests. The difference in generation methods could cause differences in bubble size and count or addition of peroxide could alter the clay chemistry. Either phenomenon could lead to different bubble release behaviors. Second, the test containers have different aspect ratios. Scoping tests used wide (~20 cm) 2 L beakers, whereas current testing used a 5 cm (diameter) column. It is possible that the increased bubble-wall interactions in the current testing could alter the release behavior. Finally, scoping and current gas release tests use different release mechanisms. Scoping tests disrupted bubbles by stirring with a spatula (~1 cm wide), whereas current tests used a vibrating table. Differences in the amplitude of disruption (up to ±100 mm with the spatula versus ±1 mm with the table) and frequency of disruption (~1 Hz with the spatula stirring versus ~50 Hz with the table) could lead to different release behaviors. Whatever the cause, the results of 50 torr vacuum testing provided motivation to perform the confirmatory tests with peroxide discussed in Section 5.4 of this report.

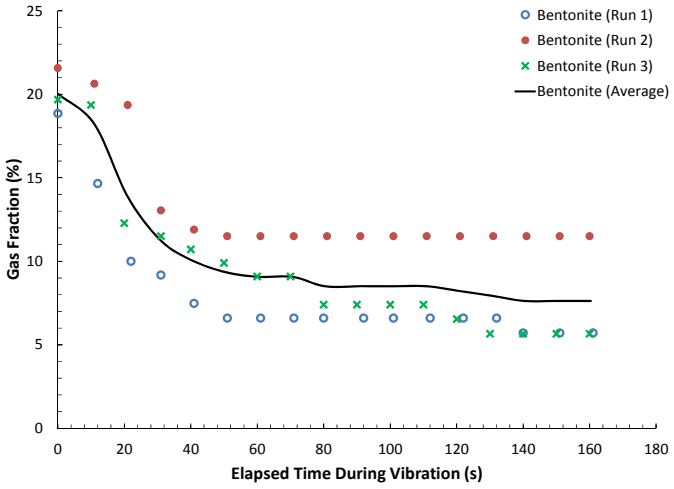

(A)

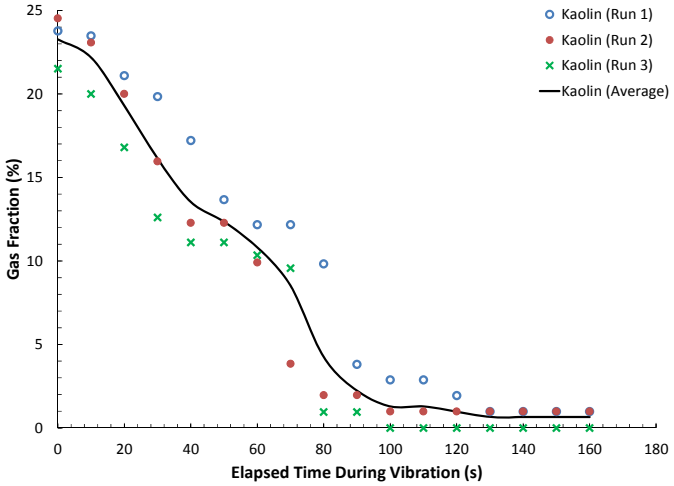

(B)

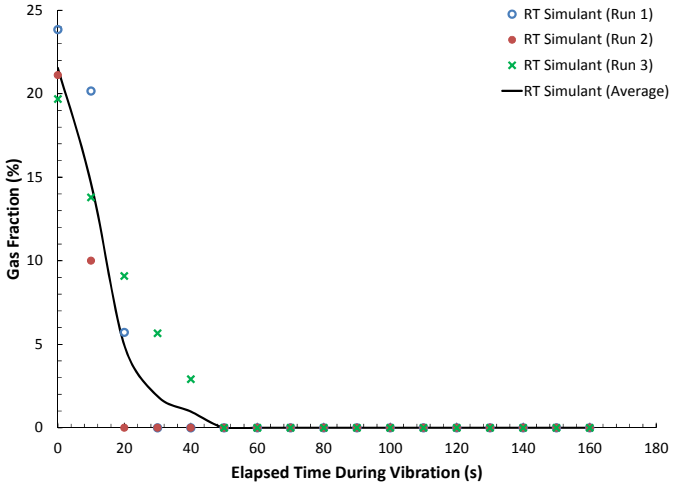

(C)

Figure 5.4. Release of Gas Upon Vibration in (A) 30 Pa Bentonite Clay, (B) 30 Pa Kaolin Clay, and (C) 30 Pa RT Simulant. Tests operated at constant pressure (50 torr).

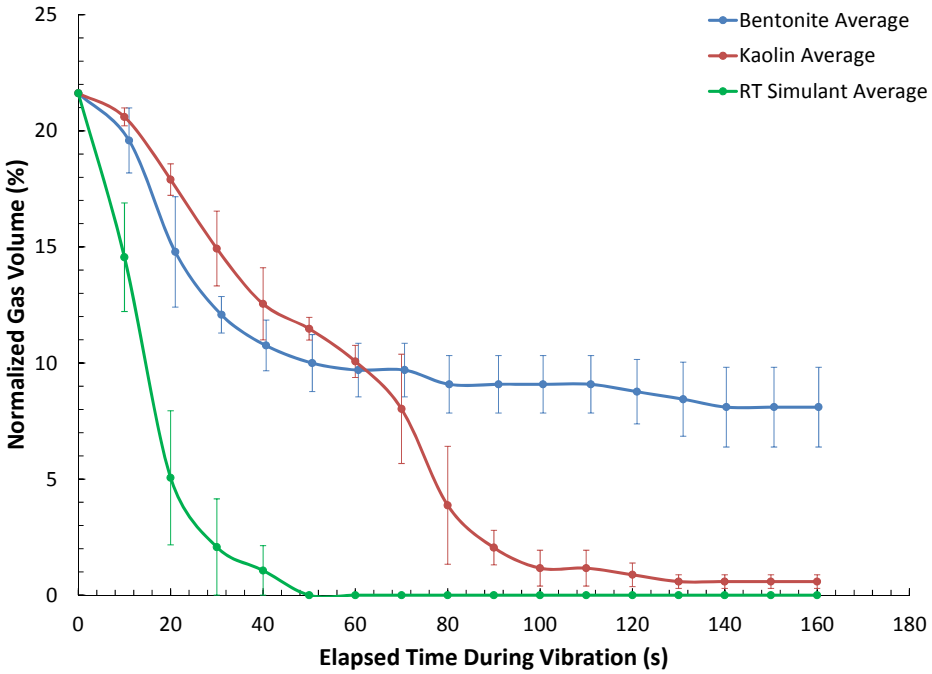

Figure 5.5. Summary of Averaged and Normalized (to 21.7 vol%, which is the global average of all initial gas fractions achieved at 50 torr vacuum) Gas Release Profiles For All Simulants. Error bars indicate standard error (which is the standard deviation divided by the square root of the number of measurements).

The results presented above (Figure 5.2 through Figure 5.5) describe bubble generation as well as the rate and extent of release, but do not describe the actual morphology of release. Gas release mechanisms can only be gaged by bubble interactions observed at the walls. All simulants appear to show similar gas migration and release behavior under vacuum. Application of vibration appears to mobilize bubbles as a result of acoustic wave action (where the vibration of slurry or bubbles yields the material surrounding the bubble). The bubbles rise as a result of buoyancy, with the rate of rise being larger for larger bubbles. As the bubbles rise, they appear to coalesce with nearby bubbles, grow larger, and rise more rapidly. This process continues until the bubble reaches the surface of the slurry. In general, large bubbles appear to collect smaller bubbles as they rise through the slurry, and large release events appear to be caused by bubbles that originate at the bottom of the test column (where the vibrational intensity is likely the strongest given the proximity to the surface of the shaker table). Bubbles that reach the surface vary in size from several millimeters to 1 centimeter. It should be noted that the bubble-rise behavior discussed above only considers the observable behavior at the wall and may not be representative of bubble-rise morphology in the interior of the test slurry.

In 30 Pa bentonite, the coalescence, growth, and release of bubbles occur frequently during the first 60 seconds. After 60 seconds, growth of bubbles through coalescence appears to slow dramatically, and while remaining bubbles still rise under the influence of vibration and buoyancy, they do so slowly. Bubble rise in kaolin is difficult to monitor because of the opacity of the slurry and high solids content (relative to bentonite). The limited bubble coalescence and rise events that can be observed at the walls appear to be morphologically similar to those observed in bentonite. However, release from kaolin does not appear to slow after 60 seconds, but instead continues until the gas is fully released. Gas release morphology in the RT Simulant is similar to that in bentonite, save that the coalescence and release of gas

occurs rapidly, such that most of the bubble release events occur within the first 40 seconds of vibration. After the first 40 seconds, continued vibration yields limited bubble coalescence and rise in the RT Simulant. However, the volume of bubbles remaining in the RT Simulant after the initial release is insufficient to yield a dramatic change in slurry level (at least within the optical resolution of the camera).

5.3 Bubble Release at Constant Volume

Bubble tests at constant volume refer to those tests in which an entrained gas fraction of 15 vol% was targeted. The vacuum pressures needed to achieve these volumes ranged from 60 to 120 torr and, in all cases, were higher than the 50 torr vacuum pressures used in Section 5.2 testing. Figure 5.6 shows the initial gas fractions achieved for primary and replicate testing for each simulant. Gas fractions for constant volume testing ranged from 13% to 18% and are lower than those obtained in constant pressure (50 torr) testing. To achieve the entrained gas fractions shown in Figure 5.6, the vacuum pressure was slowly lowered over a period of 10 to 15 minutes, allowing the gas to nucleate and expand, until the target gas fraction was reached. Care was taken not to lower the pressure too quickly to avoid gross overshoot of the target gas fraction of 15 vol%.

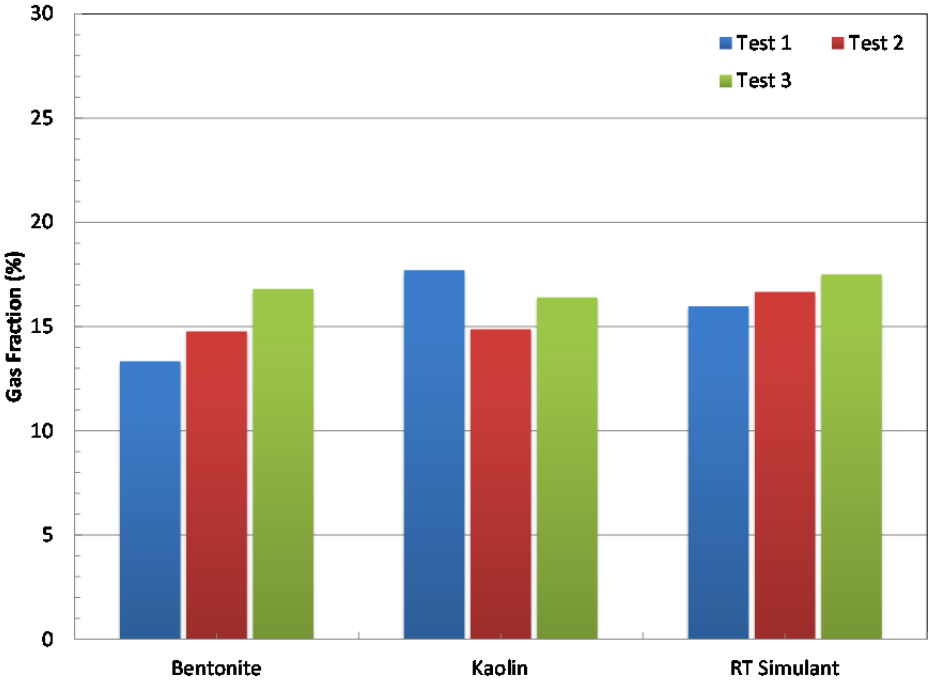

Figure 5.6. Entrained Gas Fraction Generated in Each 30 Pa Simulant for Constant Volume Testing (with a target of 15 vol% entrained gas). Test 1 is the primary test, whereas Tests 2 and 3 are the replicate tests.

Given the difference in generation time, vacuum pressure, and ultimate entrained gas fraction achieved, differences in the shape, number, and size of bubbles were expected in constant volume testing relative to constant pressure (50 torr) testing. Figure 5.7 shows select images of the bubbles generated at constant volume (15 vol%). Figure 5.7 indicates that, relative to each other, the sizes of bubbles generated in 30 Pa bentonite and 30 Pa RT Simulant are similar and larger than those generated in 30 Pa kaolin clay. For 30 Pa bentonite clay, bubbles generated at constant volume appear to be less numerous than but similar in size to those generated at 50 torr vacuum. For 30 Pa kaolin clay and 30 Pa RT Simulant, bubbles generated at constant volume appear similar to those generated at 50 torr in terms of size and count. Indeed, for 30 Pa kaolin clay and 30 Pa RT Simulant, it is difficult to determine from visual inspection of the columns if the lower entrained gas fraction achieved in constant volume testing results from smaller bubble size or lower bubble count. In contrast, visual inspection of the 30 Pa bentonite simulant suggests that lowered entrained gas fraction results primarily from reduced bubble count, rather than smaller bubble size.

Figure 5.8 shows the gas release profiles observed during primary and replicate tests for each simulant for constant volume testing. While the results obtained in constant volume testing are similar to those obtained under constant pressure (see Section 5.2), significant differences are observed in the release behavior for kaolin and the RT Simulant. For 30 Pa bentonite clay (Figure 5.8A), the primary release still occurs during the first 60 seconds of vibration. Beyond 60 seconds, the release continues at a greatly reduced rate and appears to stop slightly above 5% entrained gas volume. Overall, the release profile is similar to bentonite when gas is generated at 50 torr (and bubbles are more numerous). For 30 Pa kaolin clay (Figure 5.8B), the lower initial gas fraction (15 vol%) achieved in constant volume testing appears to slow the rate and reduce the extent of gas release from kaolin clay (relative to that observed in constant pressure testing, which exhibited an initial gas fraction of 24 vol%). At constant pressure (50 torr), the great majority of gas content in 30 Pa kaolin was released in 120 seconds. Here, gas content has been reduced to approximately 2 to 3 vol% at the end of vibration (160 seconds). From the data shown in Figure 5.8B, it is unclear if continued vibration would eventually release all the entrained gas from kaolin or if no release occurs after 2 to 3 vol% is achieved. For 30 Pa RT Simulant (Figure 5.8C), a significant release of gas is observed over the first 50 seconds of vibration; however, beyond 50 seconds, the release of gas is greatly arrested such that the entrained gas content stabilizes around 2 vol%. This observation contrasts sharply with release at higher gas fractions (e.g., those as constant pressure of 50 torr, Section 5.2), where the RT Simulant releases its gas rapidly (within 40 seconds) and completely (i.e., with no hold-up of entrained gas). For all test simulants, release of vacuum pressure caused remaining bubbles at the end of the experiment to collapse.

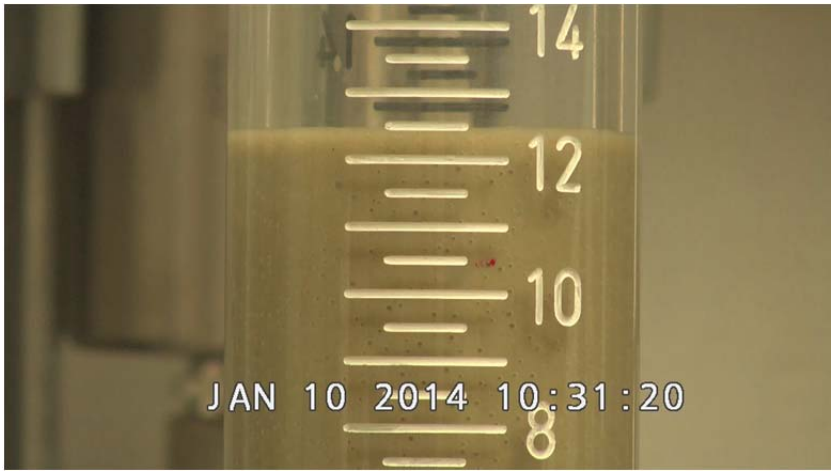

(A)

(B)

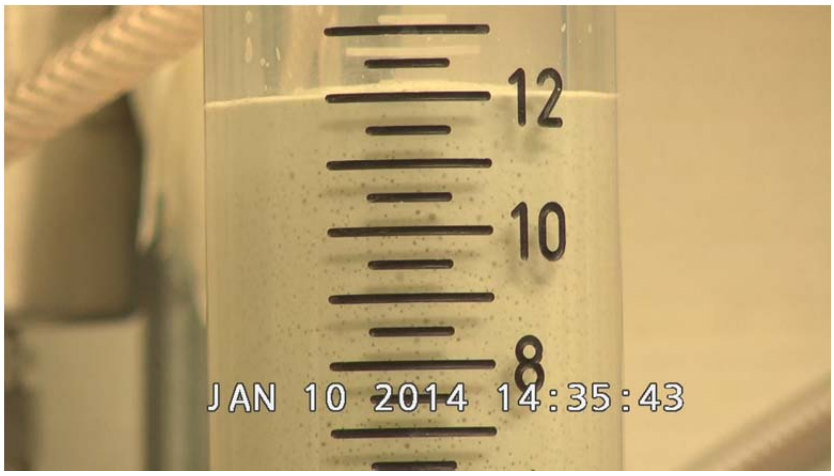

(C)

Figure 5.7. Select Images of Bubbles Generated at 15 vol% (bubble generation time ~10 minutes) in (A) 30 Pa Bentonite Clay, (B) 30 Pa Kaolin Clay, and (C) 30 Pa RT Simulant. (Note: Column height is in centimeters.)

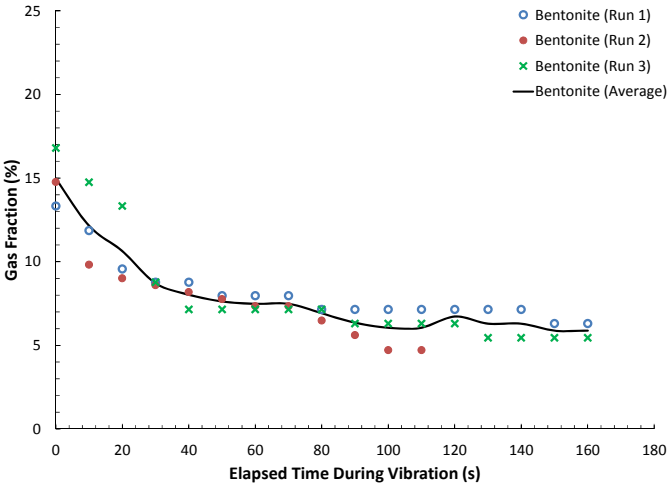

(A)

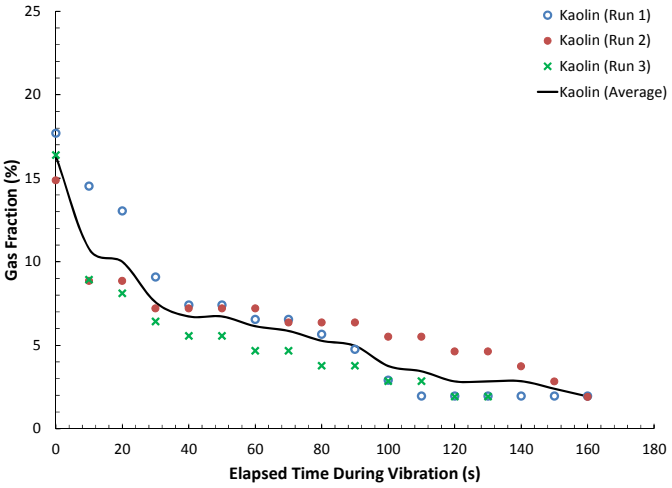

(B)

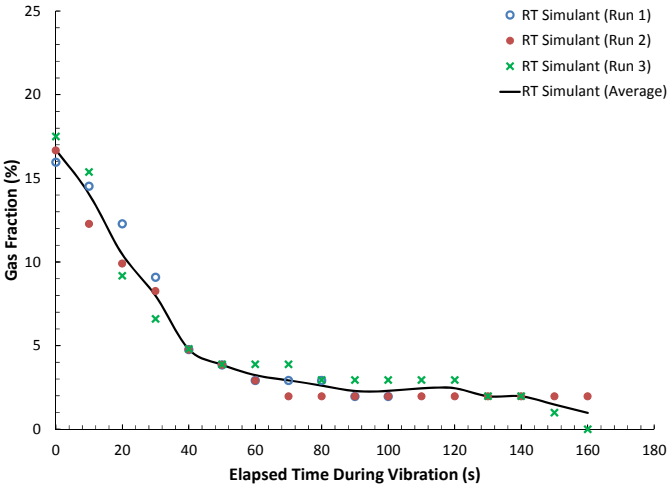

(C)

Figure 5.8. Release of Gas Upon Vibration in (A) 30 Pa Bentonite Clay, (B) 30 Pa Kaolin Clay, and (C) 30 Pa RT Simulant. Tests conducted at constant gas volume (target 15 vol%).

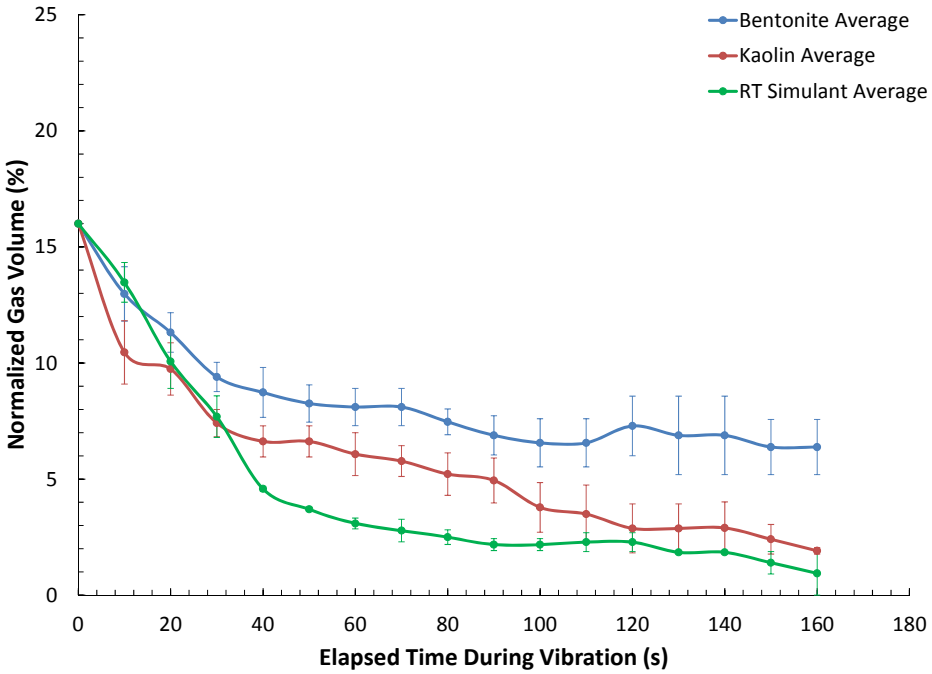

Figure 5.9. Summary of Averaged and Normalized (to 16.0 vol%, which is the global average of all initial gas fractions achieved at constant gas volume testing) Gas Release Profiles For All Simulants. Error bars indicate standard error (which is the standard deviation divided by the square root of the number of measurements).

Figure 5.9 shows the averaged normalized gas release profiles for each simulant at constant volume testing. To facilitate simulant-to-simulant comparisons, all gas fractions are normalized to 16.0 vol%, which is the global average of all primary and replicate tests for all simulants. The results shown in Figure 5.9 confirm the general release behavior observed in constant pressure testing; namely, that bentonite shows the greatest degree of gas hold-up, kaolin shows intermediate hold-up, and the RT Simulant shows the lowest hold-up. The initial gas release rates of all simulants appear similar at 15 vol%, but the extent of entrained gas hold-up diverges after 30 to 40 seconds of vibration. Relative to tests at higher gas fractions (see Figure 5.5), there are significant differences in the release behavior. Specifically, the releases in kaolin and RT Simulant are not complete at lower gas fractions. The reduced release behavior can be rationalized in terms of either reduced bubble size or count. Fewer bubbles reduces the opportunity for bubble coalescence. Since coalescence appears to drive the increase in growth and therefore the buoyant rise and release of bubbles from the test simulants, a reduction in coalescence should also reduce gas release from the simulant. A reduction in bubble size could also effect a similar reduction in coalescence, but would also hinder release through a reduced buoyant force for bubble rise (i.e., small bubbles will rise more slowly). Note that visual inspection of the bubbles during release during constant volume testing indicates a similar morphological mechanism for bubble release (i.e., coalescence and bubble rise upon vibration).

5.4 Bubble Generation with Hydrogen Peroxide

Gas generation and release testing with hydrogen peroxide involved three separate tests: 1) stir tests in 2 L beakers, 2) vibration tests in the primary test apparatus (Figure 4.1), and 3) vibration tests in a

100 mL graduated cylinder. Figure 5.10 shows the initial gas fraction generated by reaction with hydrogen peroxide for each of the test containers. The initial gas fraction for hydrogen peroxide testing ranges from 12 to 16 vol%, and as such, is similar to gas fractions realized in constant volume testing (Section 5.3). When executing vibration testing in the primary test apparatus, kaolin and bentonite clay experienced significant surface disruption that splashed clay onto the upper wall of the container. While the 30 Pa bentonite clay slurry was sufficiently transparent to still resolve the surface level, the surface level of 30 Pa kaolin clay slurry could not be resolved during vibration. As such, the gas release profile for kaolin clay is not available for the primary test column.

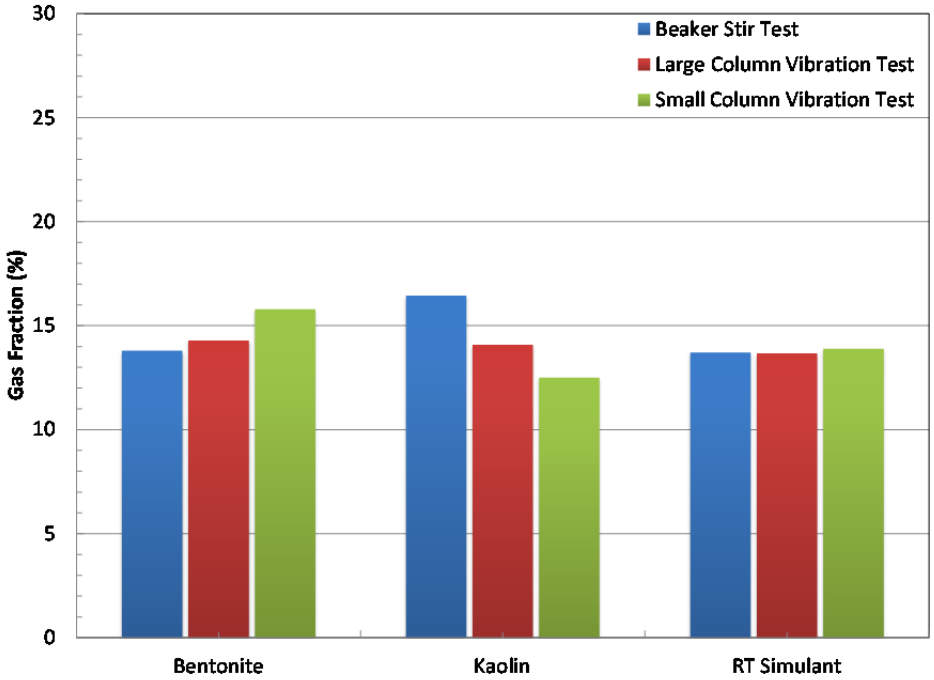

Figure 5.10. Initial Gas Fraction for Gas Generation and Release Testing with Hydrogen Peroxide

Stir tests in the 2 L beaker were captured by video from above. While no gas release profiles are available, initial and final levels were recorded. Table 5.4 shows the initial and final gas fractions observed in hydrogen peroxide stir testing. Figure 5.11 shows the surface view of each of the three test simulants before and after stir testing. The results for 2 L stir testing are consistent with the scoping tests that motivated gas generation and release morphology testing, namely that bentonite clay rapidly and completely releases entrained gas, whereas kaolin clay does not fully release its gas. Gas release from 30 Pa bentonite clay is rapid: approximately 1 minute of stirring reduces the entrained gas fraction from 13.8 to 1 vol%. In contrast, stirring does release gas from 30 Pa kaolin clay, but the degree of release is much less than bentonite. Over 1 minute of stirring, the entrained gas fraction is reduced from 16.4 to 11.6 vol%. To confirm this behavior, a replicate measurement of 30 Pa kaolin clay was performed. In replicate testing, the initial gas fraction after 16 hours of gas generation was only 10.3 vol%. Stirring of the 30 Pa kaolin slurry with 10.3 vol% gas did not release additional gas. Finally, the extent of gas release from the RT Simulant falls in between kaolin and bentonite clays. Specifically, 1 minute of stirring reduces the entrained gas from 13.7 to 7.1 vol%.

Table 5.4. Gas Fractions for 2 L Beaker Hydrogen Peroxide Stir Testing Before and After Stirring

Simulant	Stir Duration (seconds)	Initial Gas Fraction (%)	Gas Fraction After Stirring (%)
30 Pa bentonite clay	51	13.8	1.0
30 Pa kaolin clay (Initial)	61	16.4	11.6
30 Pa kaolin clay (Replicate)	60	10.3[(a)]	10.3
30 Pa RT Simulant	75	13.7	7.1

(a) Initial gas fraction lower than expected; spontaneous release of gas before testing is suspected).

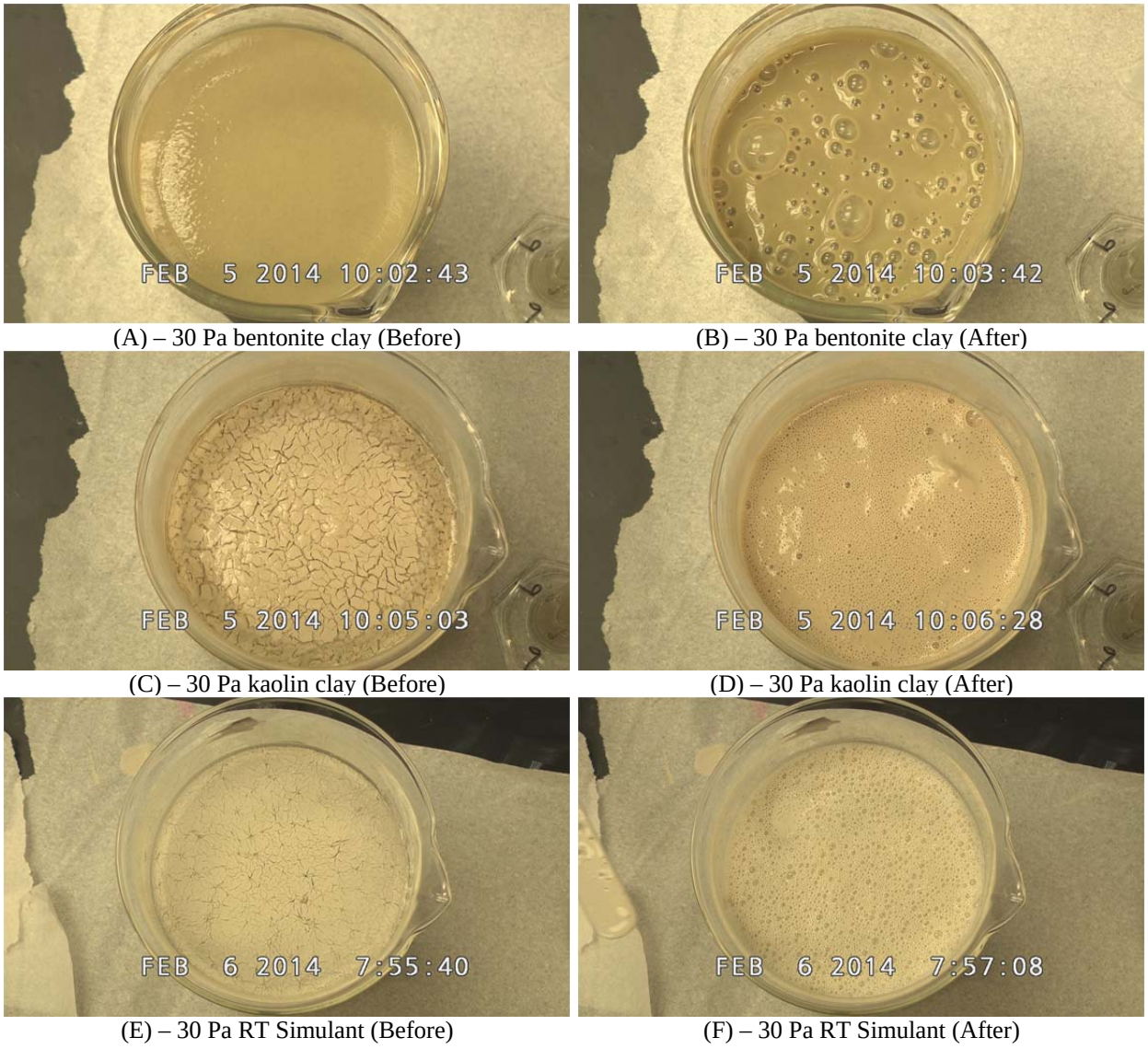

(A) – 30 Pa bentonite clay (Before)
(B) – 30 Pa bentonite clay (After)
(C) – 30 Pa kaolin clay (Before)
(D) – 30 Pa kaolin clay (After)
(E) – 30 Pa RT Simulant (Before)
(F) – 30 Pa RT Simulant (After)

Figure 5.11. Surface Images of Simulant During Stir Testing in the 2 L Beaker: (A) 30 Pa Bentonite Clay Before Stirring, (B) 30 Pa Bentonite Clay After Stirring, (C) 30 Pa Kaolin Clay Before Testing, (D) 30 Pa Kaolin Clay After Stirring, (E) 30 Pa RT Simulant Before Stirring, and (F) 30 Pa RT Simulant After Stirring. Note: The beaker diameter is 13 cm.

As suggested by the results in Table 5.4, the morphology of gas release from simulants where entrained gas is generated by hydrogen peroxide is different from that observed in vacuum testing. In vacuum testing, generation and release occurs shortly (within minutes) after loading the simulant into the column. When testing with hydrogen peroxide, the simulant sits for approximately 16 hours to allow for sufficient peroxide decomposition to produce 15 vol%. The long reaction time was selected in an attempt to produce "mature" (i.e., large) gas pockets. Use of hydrogen peroxide does not appear to impact bentonite clay; the surface image of the clay before stirring (Figure 5.11A) suggests a uniform slurry. Side images of the slurry in the primary test column show that the bubble morphology produced by hydrogen peroxide is similar to that produced by application of vacuum (cf. Figure 5.12A and Figure 5.7A). On the other hand, the surface image of 30 Pa kaolin clay slurry before stirring (Figure 5.11C) indicates dewatering and cracking of the slurry. Side images in the primary test column find less extensive cracking (presumably by entrained gas) of the slurry than evidenced by the surface. Cracks that appear at the wall of 30 Pa kaolin appear to radiate from gas bubbles generated by hydrogen peroxide decomposition. The bubble morphology in 30 Pa RT Simulant (Figure 5.11E) is similar to that in kaolin. However, simulant cracking in the RT Simulant is less frequent than in 30 Pa kaolin clay. In addition to cracking, both kaolin and RT Simulant dewater, such that a layer of surface water covers the top of the test slurry. It is postulated that dewatering results from settling of the slurry solids during the 16 hours needed to reach the target gas concentration, reaction of peroxide with the simulant solids, or some combination thereof.

In all cases, stirring of the simulant appears to homogenize the slurry such that cracks and dewatered layer are no longer visible. Release of gas from simulants reacted with hydrogen peroxide is also unique, relative to vacuum testing of simulants, in that semi-stable bubbles are formed that do not immediately burst when they reach the surface of the simulant. For 30 Pa bentonite (see Figure 5.11B), bubbles that reach the surface are large and ~1 cm in diameter. For both 30 Pa RT Simulant and kaolin clay (see Figure 5.11D and Figure 5.11F), bubbles that reach the surface are small (1 to 5 mm) and form a stable foam that covers the surface of the slurry. The foam formed by stirring kaolin is especially robust, and resists breakage on continued stirring and can last for several hours after testing. As discussed in the following pages, formation of stable bubbles is also observed in the hydrogen peroxide vibration testing. Bubbles that reach the foam layer are considered "released" and the thickness of the foam layer is not included in the simulant height when estimating the gas release profile.

Figure 5.12 shows the morphology of entrained gas formed by decomposition of hydrogen peroxide in all three simulants when tested in the primary test column. Bubbles formed by hydrogen peroxide decomposition in 30 Pa bentonite appear identical to those formed by application of vacuum (see Figure 5.3A and Figure 5.7A). Hydrogen peroxide decomposition forms bubbles in 30 Pa kaolin and 30 Pa RT Simulant that appear similar to those formed by application of vacuum; however, bubble formation by hydrogen peroxide is accompanied by a small degree of radial cracking and/or slit formation. The degree of crack formation is more severe in kaolin clay. As discussed above, the side profiles of both kaolin clay and RT Simulant evidence dewatering and/or settling of slurry solids.

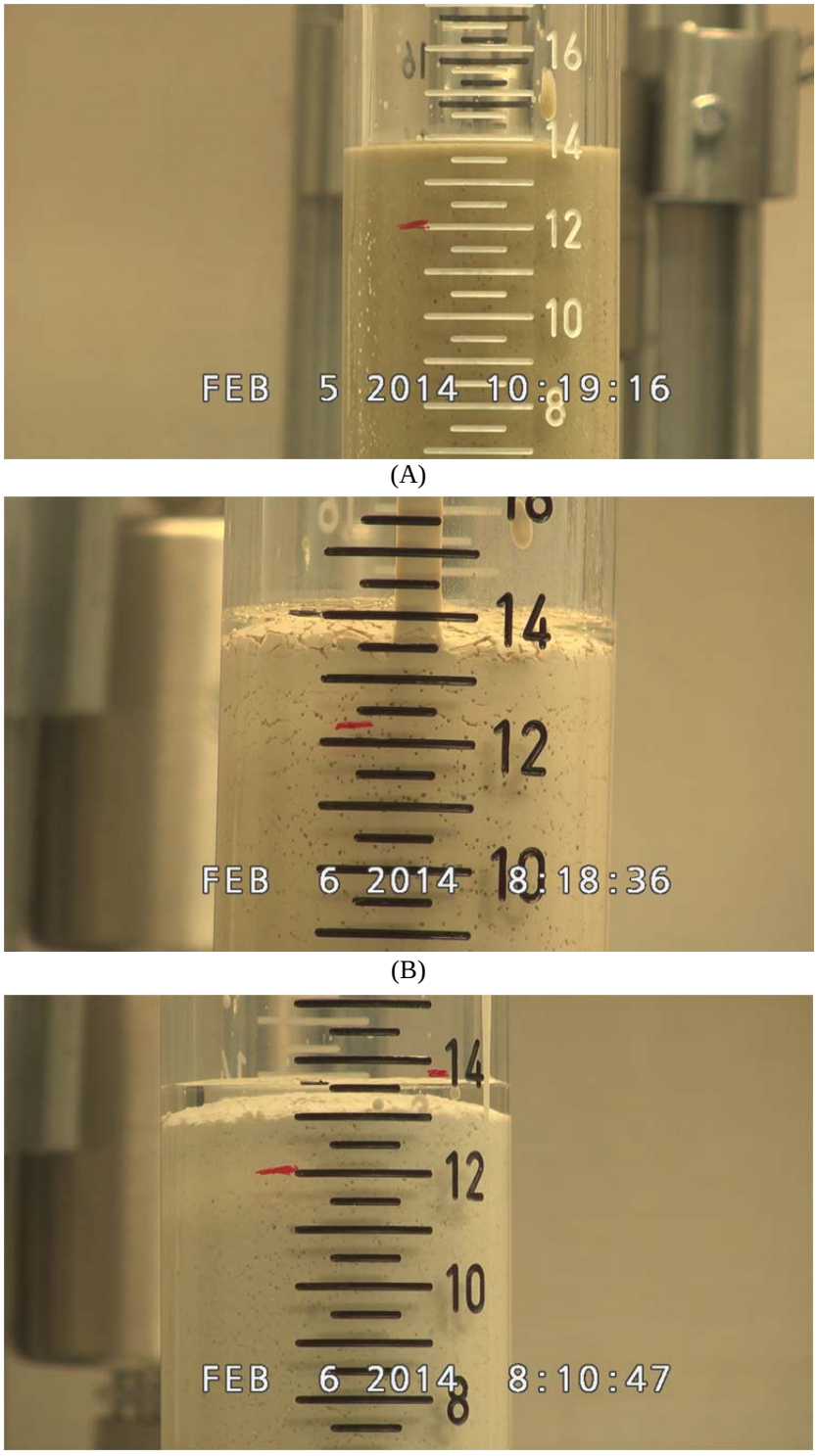

Figure 5.12. Select Images of Bubbles Generated by Hydrogen Peroxide in the Primary Test Column: (A) 30 Pa Bentonite Clay, (B) 30 Pa Kaolin Clay, and (C) 30 Pa RT Simulant. Note: Column height is in centimeters.

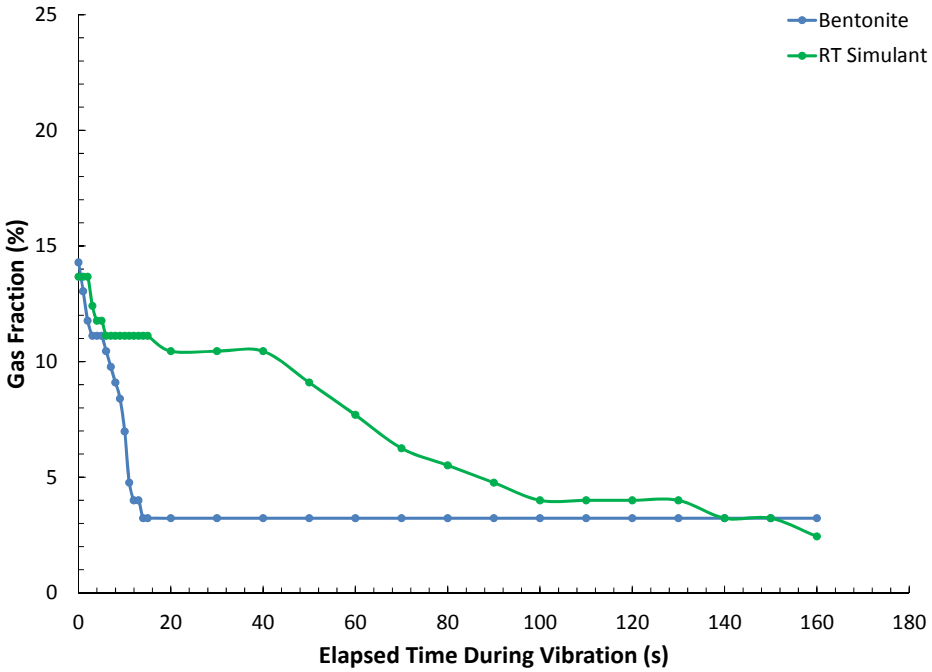

Figure 5.13. Release of Gas Generated by Hydrogen Peroxide in the Primary Test Column Using Vibration. Results for 30 Pa kaolin clay are not available because vibration splashed slurry onto the clear acrylic walls (in both a primary and a replicate test), preventing assessment of slurry level change with time.

Figure 5.13 shows the release profiles for gas, generated by hydrogen peroxide decomposition, in the primary test apparatus. Results for 30 Pa kaolin could not be obtained because vibration causes surface disruption and splashing of simulant onto the test container, obscuring change in the surface level of the kaolin slurry during gas release. As such, only results for 30 Pa bentonite and 30 Pa RT Simulant are shown in Figure 5.13. Gas release profiles in the primary test apparatus indicate a rapid initial release from 30 Pa bentonite. Specifically, over the first ~15 seconds of vibration, the entrained gas fraction in bentonite clay drops from 14 to 3 vol%. No further release of gas occurs after this initial release from bentonite. The final gas hold-up in bentonite is larger than that observed in stir testing, but less than that observed in vacuum testing (see Sections 5.2 and 5.3). For 30 Pa RT Simulant, the release over the first 5 seconds of vibration is similarly rapid to that of bentonite; however, this initial release only reduces the entrained gas fraction from 14 to 11 vol%. The release process in RT Simulant is arrested for approximately 30 seconds following this initial rapid release. Continued vibration then effects a slow release whereby the entrained gas in RT Simulant is reduced from 11 to 3 vol% over 100 seconds. At the end of the vibration period, the final hold-up of gas in RT Simulant (3 vol%) is similar to that in bentonite. These results are consistent with those of the stir test (see Table 5.4). That is, gas bubbles generated by hydrogen peroxide appear to more readily release from bentonite relative to RT Simulant. Although stir and vibration tests show differences in the ultimate extent of release by RT Simulant, this observation is not necessarily unexpected as the two techniques use different methods to release bubbles (i.e., stirring versus vibration) and different disruption durations (60 seconds of stirring versus 160 seconds of vibration).

Figure 5.14 shows the retained gas structure for gas generated by hydrogen peroxide in the 100 mL graduated cylinder. The initial gas morphology is similar to that observed in the primary test apparatus: gas bubbles are formed in 30 Pa bentonite whereas gas bubbles with radial cracks are formed in 30 Pa kaolin and RT Simulant (with kaolin showing the most extensive crack formation). Figure 5.15 shows the gas release profile for the three simulants for hydrogen peroxide testing in the 100 mL graduated cylinder. The 30 Pa bentonite and 30 Pa RT Simulant results mirror those for the primary test apparatus (see Figure 5.13). Specifically, bentonite experiences a rapid release, where the entrained gas fraction drops from 16 to 6 vol%, over the first 15 seconds. Continued vibration slowly expels gas over the next 60 seconds until the gas fraction ultimately reaches 3 vol% at the end of vibration. For 30 Pa RT Simulant, gas is released more slowly but reaches the same extent of release (~2 vol%) after 100 seconds of vibration. Testing of the 30 Pa kaolin clay slurry in the 100 mL graduated cylinder and at the lower vibration amplitude setting of 4 (relative to 8 in the primary column) did not evidence the same surface disruption and splashing experienced in the primary test column. In the 100 mL cylinder, gas release from 30 Pa kaolin was slow relative to bentonite and RT Simulant. Specifically, the primary gas release event from 30 Pa kaolin occurs during the first 60 seconds of vibration and reduces the gas content from 12.5 to 10 vol%. Continued vibration does not substantially expel more gas from kaolin, and at the end of the 160-second vibration period, the entrained gas fraction in 30 Pa kaolin is still 8 vol%. Similar results were found in stir testing, where the final gas fraction in the stirred 2 L beaker of 30 Pa kaolin was ~12 vol%. In relative terms, the 100 mL graduated cylinder tests are consistent with the 2 L beaker stir tests in that they indicate that 30 Pa bentonite releases gas rapidly and to a significant extent (although not completely) when disturbed and that 30 Pa kaolin exhibits minimal and slow gas release upon disruption. In relative terms, gas release from 30 Pa RT Simulant falls between bentonite and kaolin release in terms of rate. The ultimate extent of gas release from 30 Pa RT Simulant is similar to, if not slightly greater than, that observed for 30 Pa bentonite clay.

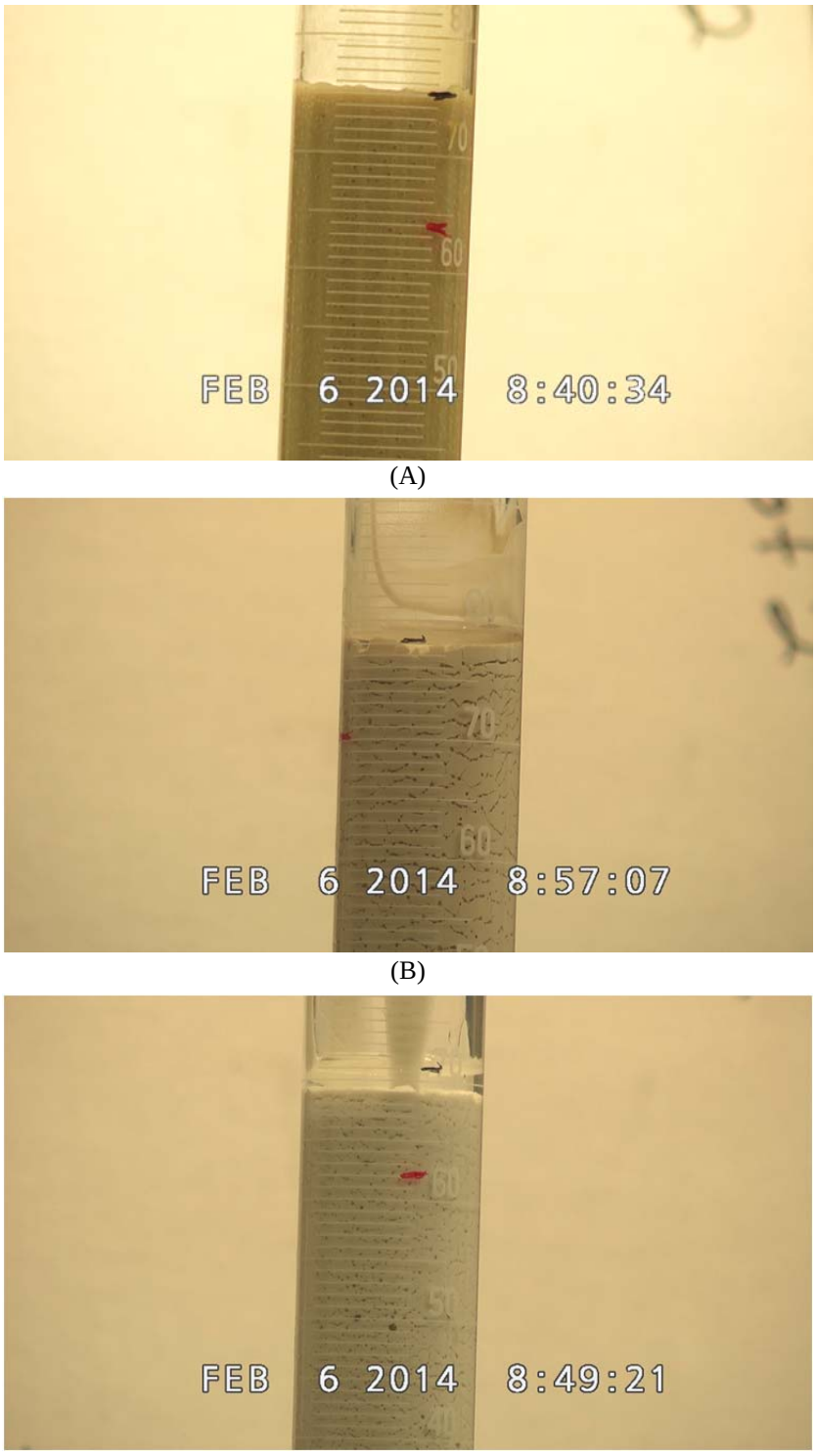

Figure 5.14. Select Images of Bubbles Generated by Hydrogen Peroxide in the 100 mL Graduated Cylinder: (A) 30 Pa Bentonite Clay, (B) 30 Pa Kaolin Clay, and (C) 30 Pa RT Simulant. Note: Cylinder markers indicate volume in milliliters. The cylinder diameter is ~3 cm. All simulants were tested at a vibration intensity of 4.

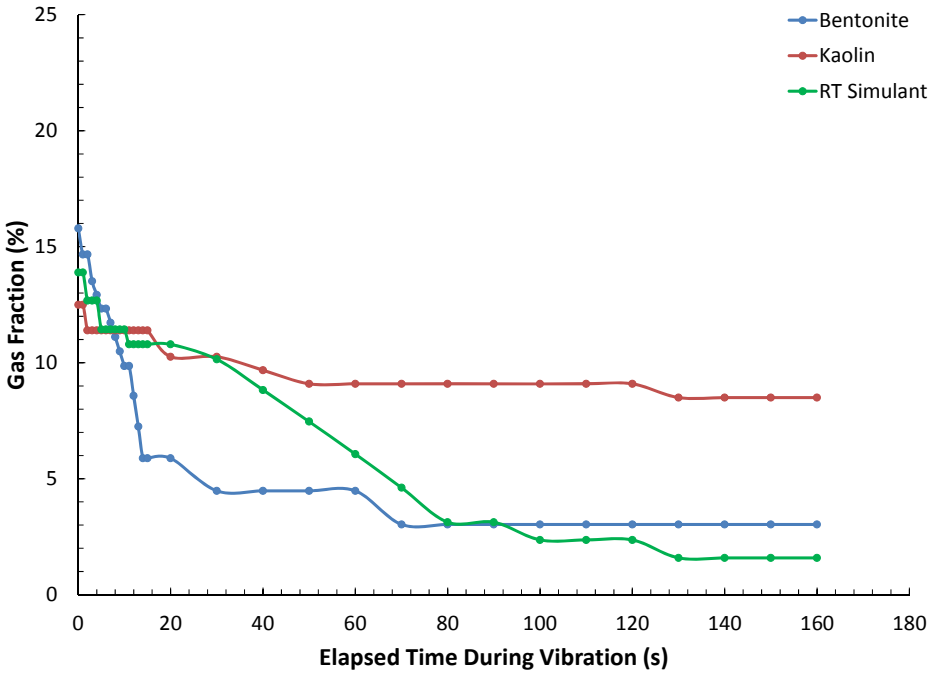

Figure 5.15. Release of Gas Generated by Hydrogen Peroxide in the 100 mL Graduated Cylinder Using Vibration

6.0 Summary

This report documents testing activities conducted as part of the Deep Sludge Gas Release Event Project (DSGREP). The testing described in this report supports evaluations of the potential retention and release mechanisms of hydrogen bubbles in underground radioactive waste storage tanks at Hanford. The primary goal of the testing was to evaluate the rate, extent, and morphology of gas release in simulant materials. Previous, undocumented scoping tests have shown dramatically different gas release behaviors from simulants with similar physical properties. Specifically, previous gas release tests have evaluated the extent of release of 30 Pa kaolin and 30 Pa bentonite clay slurries. While both materials are clays and both have equivalent material shear strength using a shear vane, it was found that upon stirring, gas was released immediately and completely from bentonite clay slurry while little if any gas was released from the kaolin slurry. The current work replicated the undocumented kaolin and bentonite clay tests in a controlled quality test environment and evaluated gas release in another simulant recently used in DSGREP testing. Overall, three simulant materials were evaluated: 1) a 30 Pa kaolin clay slurry, 2) a 30 Pa bentonite clay slurry, and 3) Rayleigh-Taylor (RT) Simulant (a simulant designed to support DSGREP RT instability testing[1]). Entrained gas was generated in the simulant materials using two methods: 1) application of vacuum over about a 1-minute period to nucleate dissolved gas within the simulant and 2) addition of hydrogen peroxide to generate gas by peroxide decomposition in the simulants over about a 16-hour period. Bubble release was effected by vibrating the test material using an external vibrating table. When testing with hydrogen peroxide, gas release was also accomplished by stirring of the simulant.

Table 6.1 provides the matrix of tests supporting the test activities documented in this report. For tests where gas was generated by application of vacuum, two test strategies were employed: one where bubbles were grown at 50 torr (to whatever ultimate gas fraction could be achieved at this vacuum pressure) and another where bubbles were grown until the total fraction of entrained gas was approximately 15%. Gas fractions generated using 50 torr vacuum ranged from 18 to 24 vol%, whereas gas fractions in experiments targeting 15 vol% entrained gas realized gas fractions ranged from 13 to 18 vol%. Tests performed under vacuum with vibration as the primary means of gas release found that all simulants partially release entrained gas. However, bentonite clay demonstrated strong retention of approximately 5% to 10% gas after the primarily release. Vibration removed the bulk of entrained gas from kaolin clay, where RT Simulant typically showed rapid and near complete release of gas relative to the other two simulants. In all cases, gas release appeared to be affected by bubble coalescence, which allowed the bubbles to grow and rise more rapidly (under the influence of buoyancy) through the test material. Large releases were observed to correspond with the rise of bubbles from the bottom of the test collection. The results indicated that gas release was more complete when the initial fraction of gas entrained in the slurry is high. Increased gas content is postulated to favor bubble coalescence, which drives the release process, as well as provide more extensive shearing of the slurry, leading to greater shear-induced motion and release of bubbles (similar to that observed in bubble cascade release events.

[1] Rassat SD, PA Gauglitz, LA Mahoney, RP Pires, DR Rector, JA Fort, GK Boeringa, DN Tran, MR Elmore, and WC Buchmiller. 2013. *Gas Release Due to Rayleigh-Taylor Instability within Sediment Layers in Hanford Double-Shell Tanks: Results of Scaled Vessel Experiments, Modeling, and Extrapolation to Full Scale*. PNNL-23060 (DSGREP-RPT-002, Rev. 0), Pacific Northwest National Laboratory, Richland, Washington.

The observed bubble release behavior under vacuum was different from the results of the scoping tests that motivated the current test activities. Specifically, scoping tests with bubbles generated by hydrogen peroxide decomposition found near-complete release of gas from 30 Pa bentonite clay and retention of gas by 30 Pa kaolin clay. Current tests with bubbles generated by application of vacuum found near complete release of gas from kaolin and only partial release of gas from bentonite. There are several differences in the scoping and DSGREP bubble release tests that could give rise to the difference in gas release behaviors. The difference in generation methods could explain differences in bubble size and count or addition of peroxide could alter the simulant chemistry. Either phenomenon could lead to different bubble release behaviors. Second, the test containers have different aspect ratios. Scoping tests used wide (~20 cm) 2 L beakers, whereas current testing used a 5 cm (internal diameter) column. It is possible that the increased bubble-wall interactions in the current testing altered the release behavior. Finally, scoping and current gas release tests used different release mechanisms. Scoping tests disrupted bubbles by stirring with a spatula (~2.5 cm wide), whereas current tests used a vibrating table. Differences in the amplitude of disruption (up to ±100 mm with the spatula versus ±1 mm with the table) and frequency of disruption (~1 Hz with the spatula stirring versus ~50 Hz with the table) could lead to different release behaviors. Whatever the cause, the results of 50 torr vacuum testing provided motivation to perform the confirmatory tests with peroxide discussed in Section 5.4 of this report.

To determine the cause of the discrepancy between gas release behaviors in scoping tests and the vacuum tests, gas generation and release tests in all three simulants were repeated using hydrogen peroxide as the gas generation mechanism. These tests confirmed the release behavior observed in the scoping tests that motivated the current test activities. Specifically, the hydrogen peroxide tests indicate that, when bubbles are formed using hydrogen peroxide decomposition over long growth periods (i.e., 16 hours) to a target initial gas fraction of 15 vol%, shear or vibration of:

- 30 Pa bentonite clay slurry releases gas immediately and to a significant, but not complete, extent (with final gas hold-up ranging from 1 to 3 vol%)
- 30 Pa kaolin clay slurry releases gas slowly and to a minimal extent (with final gas hold-up ranging from 8 to 12 vol%)
- 30 Pa RT Simulant effects a release that, in terms of rate, falls between that of kaolin and bentonite, and that, in terms of extent, is comparable to that of bentonite.

As discussed above, there are several differences in vacuum and hydrogen peroxide release tests that could cause the difference in gas release behaviors. First, the difference in gas generation methods could give release to differences in bubble size distribution and count or addition of peroxide could alter the simulant chemistry/rheology. Observation of bubbles at the wall appears to confirm that hydrogen peroxide produces an entrained gas morphology different from vacuum testing, at least in 30 Pa kaolin and 30 Pa RT Simulant. Specifically, use of hydrogen peroxide produced spherical bubbles with radial cracks[1] in kaolin and RT Simulant, whereas use of a vacuum only produces small (on the order of 1 mm and smaller), spherical bubbles. In addition, both 30 Pa kaolin and RT Simulant dewatered when testing with hydrogen peroxide; it is postulated that dewatering results from solids settling over the long bubble growth period (16 hours in hydrogen peroxide testing relative to 1 to 15 minutes in vacuum testing), from reaction of the clay with peroxide, or from some combination of these two effects. Use of hydrogen

[1] Visual observation was unable to determine if the cracks were filled with gas or water.

peroxide did not noticeably alter bubble morphology in bentonite clay relative to vacuum testing; both methods produce only small spherical bubbles. Use of hydrogen peroxide did not appear to drastically alter the shear strength of the test materials. Shear strength measurements were made on simulants with added hydrogen peroxide immediately before disruption; all fell within the acceptable test range of 15 to 45 Pa and were generally around 20 to 30 Pa.

Table 6.1. Matrix of Bubble Generation and Release Studies for Gas Generation and Release Morphology Testing

Simulant Material	Gas Generation Method	Test Vessel	No. of Tests
30 Pa kaolin	Vacuum (at 50 torr)	Sealed Test Column	3
	Vacuum (to 15% Gas Volume)	Sealed Test Column	3
	Hydrogen Peroxide	2 L Beaker	1
	Hydrogen Peroxide	Primary Test Apparatus	1
	Hydrogen Peroxide	100 mL Graduated Cylinder	1
30 Pa bentonite	Vacuum (at 50 torr)	Sealed Test Column	3
	Vacuum (to 15% Gas Volume)	Sealed Test Column	3
	Hydrogen Peroxide	2 L Beaker	1
	Hydrogen Peroxide	Primary Test Apparatus	1
	Hydrogen Peroxide	100 mL Graduated Cylinder	1
30 Pa RT Simulant	Vacuum (at 50 torr)	Sealed Test Column	3
	Vacuum (to 15% Gas Volume)	Sealed Test Column	3
	Hydrogen Peroxide	2 L Beaker	1
	Hydrogen Peroxide	Primary Test Apparatus	1
	Hydrogen Peroxide	100 mL Graduated Cylinder	1
Total			27

It could also be postulated that differences in the geometry of the test container or method of gas release (vibration versus stirring) yield the differences in release behavior observed between hydrogen peroxide and vacuum testing. Specifically, scoping tests used wide (~20 cm) 2 L beakers with stirring as the release mechanism, whereas current vacuum testing used a 5 cm (internal diameter) column with vibration as a gas release mechanism. To evaluate the influence of test container geometry and release mechanism on gas release, hydrogen peroxide tests were repeated in the primary test apparatus (used for vacuum testing) and in a smaller-diameter 100 mL graduated cylinder, with bubble release effected by vibration. In general, these tests found that the gas release behaviors did not depend strongly on test container geometry or on release mechanism (vibration versus stirring) such that the gas release profiles mirrored those for the 2 L hydrogen peroxide stir tests.

For these reasons, it can be postulated that the difference in release behaviors observed between vacuum and hydrogen peroxide testing primarily derives from the method of gas generation itself (and how nucleation of dissolved gas or decomposition of hydrogen peroxide impacts local simulant chemistry) or on the length of time required to grow bubbles (several minutes using vacuum versus up to 16 hours when using hydrogen peroxide). In terms of shear strength, several differences are notable between vacuum and hydrogen peroxide testing. For vacuum testing, shear strength is similar among test

simulants, and here, the strongest simulant, kaolin at ~25 Pa, releases more completely than the relatively weaker ~18 Pa bentonite slurry. When testing with hydrogen peroxide, bentonite clay slurry shear strength (which at 22 Pa is nearly unchanged relative to that realized in vacuum testing) falls below that measured for kaolin (36 Pa) and RT Simulant (38 Pa). The cause of increase in the shear strength of kaolin and RT Simulant slurries over that achieved in vacuum testing can be attributed to reaction of the simulant with hydrogen peroxide or, more likely, by compaction (and increased solids concentration of the slurry) as a result of settling and dewatering. In terms of observed gas release behaviors, the weakness of the bentonite slurry in hydrogen peroxide testing (relative to kaolin and RT Simulant) could explain the rapid release of entrained gas from bentonite relative to other test simulants. However, reliance on shear strength alone does not explain why the similar strength bentonite slurry does not release rapidly or to the same extent in vacuum testing, nor does it explain why the 38 Pa RT Simulant releases more quickly and to greater extent than the 36 Pa kaolin slurry when testing with hydrogen peroxide. As such, while material strength may play a role in the release behavior, other equally important mechanisms appear to control that rate and extent of gas release.

It is expected that different gas generation and growth mechanisms (i.e., vacuum versus hydrogen peroxide) will result in different entrained bubble count, morphology, and size. Qualitative analysis of gas morphology, by observing entrained gas at the container walls, finds that vacuum testing produces spherical bubbles in all test simulants whereas hydrogen peroxide produces bubbles in bentonite slurries and bubbles with radial cracks in kaolin and RT Simulant slurries. Current assessment of bubble morphology should be approached with caution, as it presumes that the bubble morphology observed at the container walls is representative of the internal bubble morphology (which could not be visually assessed because all test slurries were opaque). Regardless of this limitation, it is likely that differences in the bubble size distribution across simulants and between gas generation methods will drive differences in the how bubbles and gas pockets coalesce with one another, rise through, and are expelled from the test simulant. Assessment of entrained gas morphology in the current study did not attempt to quantify differences in bubble count and size distribution across test simulants and gas generation methods. If resolution of the differences observed in vacuum and hydrogen peroxide release testing is needed, then future tests should consider quantification of bubble structure within the test simulant for each gas generation mechanism.

Overall, the test results presented suggest that caution should be exercised when selecting the bubble generation and simulant disturbance methods when evaluating the gas release behaviors. The results of this study indicate that bubble nucleation and growth by application of a vacuum and subsequent release by vibration do not replicate gas release behaviors obtained by hydrogen peroxide decomposition and subsequent stirring. Indeed, the gas release behaviors obtained in vacuum and vibration testing is the reverse of that obtained when testing with hydrogen peroxide. These differences suggest a strong dependence of the gas release behaviors on the mechanism used to form the bubbles in situ. Further development of simulants and gas generation mechanisms for release testing should evaluate the reasonableness of gas release morphology against that observed in actual wastes.

7.0 References

Bryan SA, LR Pederson, and RD Scheele. 1992. "Crust Growth and Gas Retention in Synthetic Hanford Waste." In *Proceedings of Waste Management '92*, pp. 829-834.

Crawford AD, SA Bryan, CA Burns, and RC Daniel. 2013. *Gas Retention and Release within Hanford Tank Waste*. PNNL-23043, Pacific Northwest National Laboratory, Richland, Washington.

Daniel RC, KJ Cantrell, RW Shimskey, JM Billing, RA Peterson, LK Jagoda, ML Luna, and ML Bonebrake. 2009. *Characterization of Filtration Scale-Up Performance.* PNNL-18117, WTP-RPT-168 Rev. 0, Pacific Northwest National Laboratory, Richland, Washington.

Epstein M and PA Gauglitz. 2010. *An Experimental Study of the Stability of Vessel-Spanning Bubbles in Cylindrical, Annular, Obround and Conical Containers.* FAI/09-272, Rev. 2, Fauske & Associates, LLC, Burr Ridge, Illinois.

Gauglitz PA, SD Rassat, PR Bredt, JH Konynenbelt, SM Tingey, and DP Mendoza. 1996. *Mechanisms of Gas Bubble Retention and Release: Results for Hanford Waste Tanks 241-S-102 and 241-SY-103 and Single-Shell Tank Simulants.* PNL-11298, UC-2030, Pacific Northwest Laboratory, Richland, Washington.

Gauglitz PA, J Chun, MM Mastor, B Buchmiller, RL Russell, JJ Jenks, and AJ Schmidt. 2010. *The Disruption of Vessel-Spanning Bubbles with Sloped Fins in Flat-Bottom and 2:1 Elliptical-Bottom Vessels.* PNNL-19345, Rev. 0, 53451-RPT08, Pacific Northwest National Laboratory, Richland, Washington.

Gauglitz PA, WC Buchmiller, SG Probert, AT Owen, and FJ Brockman. 2012. *Strong-Sludge Gas Retention and Release Mechanisms in Clay Simulants.* PNNL-21167, Rev. 0, EMSP-RPT-013, Pacific Northwest National Laboratory, Richland, Washington.

Gauglitz PA, BE Wells, SD Rassat, and WC Buchmiller. 2013. *Rayleigh-Taylor Instability within Sediment Layers Due to Gas Retention: Preliminary Theory and Experiments*. PNNL-22339, Rev. 0, Pacific Northwest National Laboratory, Richland, Washington.

Laxton PB and JC Berg. 2005. "Gel trapping of dense colloids." *Journal of Colloid and Interface Science* 285:152–157.

Powell MR, PA Gauglitz, KM Denslow, CM Fischer, MS Prowant, SA Sande, JM Davis, MR Telander, and DJ Heldebrant. 2014. *Evaluation of Gas Retention in Waste Simulants: Intermediate-Scale Column and Open-Channel-Depth Tests.* PNNL-23136, DSGREP-RPT-003, Rev. 0, Pacific Northwest National Laboratory, Richland, Washington.

Rassat SD and PA Gauglitz. 1995. *Bubble Retention in Synthetic Sludge: Testing of Alternative Gas Retention Apparatus.* PNL-10661, UC-510, Pacific Northwest Laboratory, Richland, Washington.

Rassat SD, PA Gauglitz, PR Bredt, LA Mahoney, SV Forbes, and SM Tingey. 1997. *Mechanisms of Gas Retention and Release: Experimental Results for Hanford Waste Tanks 241-AW-101 and 241-AN-103*. PNNL-11642, UC-2030, Pacific Northwest National Laboratory, Richland, Washington.

Rassat SD, PA Gauglitz, SM Caley, DE Rinehart, PR Bredt, and SV Forbes. 1998. *Mechanisms of Gas Retention and Release: Experimental Results for Hanford Single-Shell Waste Tanks 241-A-101, 241-S-106, and 241-U-103*. PNNL-11981, UC-2030, Pacific Northwest National Laboratory, Richland, Washington.

Rassat SD, PA Gauglitz, LA Mahoney, RP Pires, DR Rector, JA Fort, GK Boeringa, DN Tran, MR Elmore, and WC Buchmiller. 2013. *Gas Release Due to Rayleigh-Taylor Instability within Sediment Layers in Hanford Double-Shell Tanks: Results of Scaled Vessel Experiments, Modeling, and Extrapolation to Full Scale.* PNNL-23060, DSGREP-RPT-002, Rev. 0, Pacific Northwest National Laboratory, Richland, Washington.

Russell RL, DE Rinehart, JM Billing, HD Smith, and RA Peterson. 2009. *Development and Demonstration of Ultrafiltration Simulants*. PNNL-18090, WTP-RPT-183 Rev. 0, Pacific Northwest National Laboratory, Richland, Washington.

Stewart CW, PA Meyer, MS Fountain, CE Guzman-Leong, SA Hartley-McBride, JL Huckaby, and BE Wells. 2006. Effect of Anti-Foam Agent on Gas Retention and Release Behavior in Simulated High-Level Waste. PNWD-3786, WTP-RPT-147, Battelle--Pacific Northwest Division, Richland, Washington.

Stewart CW, LA Mahoney, CE Guzman-Leong, JM Alzheimer, ST Arm, JA Bailey, MG Butcher, SK Cooley, EC Golovich, DE Hurley, LK Jagoda, CD Johnson, WR Park, LD Reid, RW Slaugh, HD Smith, Y Su, BE Wells, C Wend, and ST Yokuda. 2007. Results from Large-Scale Testing on Effects of Anti-Foam Agent on Gas Retention and Release. PNNL-17170, WTP-RPT-156 Rev 0, Pacific Northwest National Laboratory, Richland, Washington.

Wells BE, GN Brown, EC Golovich, RL Russell, DE Rinehart, JV Crum, LA Mahoney, and WC Buchmiller. 2010a. *Hanford Sludge Simulant Selection for Soil Mechanics Property Measurement*. PNNL-19250, Pacific Northwest National Laboratory, Richland, Washington.

Wells BE, N Bauman, JJ Jenks, AD Guzman, G Boeringa, P Arduino, and PJ Keller. 2010b. *Lateral Earth Pressure at Rest and Shear Modulus Measurements on Hanford Sludge Simulants*. PNNL-19829, Pacific Northwest National Laboratory, Richland, Washington.

Zhou ZAX, and JA Zhenghe-Finch. 1998. "Effect of Surface Properties of Fine Particles on Dynamic Bubble Formation in Gas-Superstatured Systems." *Industrial and Engineering Chemistry* 37(5):1998-2004.

Distribution

No. of Copies

OFFSITE

1 M Epstein
Fauske and Associates, LLC
1118 3rd Street, #308
Santa Monica, CA 90403

1 G Terrones
Applied Physics Division (X-4)
MS: T086
Los Alamos National Laboratory
Los Alamos, NM 87545

3 Savannah River National Laboratory
Savannah River Site
Aiken, SC 29808
D Koopman
C Nash
B Wilmarth

1 RD Holtz
Civil & Environmental Engineering
University of Washington
201 More Hall, Box 352700
Seattle, WA 98195-2700

No. of Copies

ONSITE

1 **DOE Office of River Protection**

BJ Stickney	H6-60

7 **Washington River Protection Solutions**

WB Barton	S7-90
R Calmus	H8-04
JM Grigsby	S7-90
NW Kirch	R2-58
DB Little	R2-58
JE Meacham	R2-58
TL Sams	R2-52

17 **Pacific Northwest National Laboratory**

SA Bryan	P7-25
CA Burns	K4-18
AD Crawford	P7-25
RC Daniel	P7-22
PA Gauglitz (5)	K7-15
LR Hylden	P7-25
PJ MacFarlan	P7-22
LA Mahoney	K7-15
SD Rassat	K6-28
DR Rector	K7-15
PP Schonewill	P7-25
BE Wells	K7-15
Project Records	

Pacific Northwest
NATIONAL LABORATORY

Proudly Operated by **Battelle** *Since 1965*

U.S. DEPARTMENT OF
ENERGY

902 Battelle Boulevard
P.O. Box 999
Richland, WA 99352
1-888-375-PNNL (7665)
www.pnnl.gov